Determination of Potential Sites and Methods for Water Harvesting in Sinai Peninsula by the Application of RS, GIS, and WMS Techniques

Hossam H. Elewa, Ahmad M. Nosair, and Elsayed M. Ramadan

Abstract

This chapter focuses on determining optimum locations for runoff water harvesting in W. Dahab Watershed, southeastern Sinai, Egypt. A comprehensive approach involving the integration of geographic information systems (GIS), remote sensing (RS), and watershed modeling (WM) was applied through the present work to identify the potential areas for runoff water harvesting (RWH) in Wadi Dahab basin of southern Sinai, Egypt. These tools were effectively used in mapping, investigation, and modeling runoff processes. Eight thematic layers were used as a multi-decision support system (MDSS) for conducting a weighted spatial probability model (WSPM) to determine the potential areas for the RWH. These layers include the volume of the annual flood, basin area, basin length, maximum flow distance, drainage density, basin slope, overland flow distance, and basin infiltration number. The performed WSPM model was run through three different scenarios: (I) equal weights to criteria, (II) weights of criteria are proposed by authors' experience, and (III) weights are assigned by the sensitivity analysis. The resulted RWH potentiality maps classified the basin into five classes ranging from very low to very high class. According to the audited scenario (scenario 3), the major area of W. Dahab basin is categorized as of high and very high for the RWH potentiality (58.27 and 15.56% of the total watershed area, respectively). The WSPM's scenario III map gives the results in favor of the other scenarios, whether based on equal weights or those that were assumed by the authors. Four storage dams and five ground cisterns were proposed in the areas of moderate, high, and very high potentialities for the RWH to harvest runoff water and mitigate flash floods hazards.

Keywords

Sinai • Wadi dahab • Geographic information systems • Runoff water harvesting • Remote sensing • Spatial modeling

H. H. Elewa (✉)
Engineering Applications & Water Division (EAWD), National Authority for Remote Sensing & Space Sciences (NARSS), Cairo, Egypt
e-mail: elewa.hossam@gmail.com; hossam.eliewa@narss.sci.eg

A. M. Nosair
Geology Department, Faculty of Science, Zagazig University, Zagazig, Egypt

E. M. Ramadan
Water Structures Department, Faculty of Engineering, Zagazig University, Zagazig, Egypt

A. M. Negm (ed.), *Flash Floods in Egypt*, Advances in Science, Technology & Innovation,
https://doi.org/10.1007/978-3-030-29635-3_14

List of Acronyms and Abbreviations Listed in the Text

ANOVA	Analysis of Variance
ASTER	Advanced Spaceborne Thermal Emission & Reflection Radiometer
BA	Basin Area
BL	Basin Length
BS	Basin Slope
DD	Drainage Density
DEM	Digital Elevation Model
E	Degree of Effectiveness
EIA	Environmental Impact Assessment
ETM	Enhanced Thematic Mapper
GIS	Geographic Information System
GSA	Global Sensitivity Analysis
IF	Basin Infiltration Number
masl	Meter above sea level
MFD	Maximum Flow Distance
OFD	Overland Flow Distance
RS	Remote Sensing
RWH	RunoffWater Harvesting
SAM	Spatial Analysis Model
ST	Total effect, Sensitivity index
VAF	Volume of Annual Flood
V_i	A partial variance
W	Wadi (dry valley)
W_c	Criterion Weight
WMS	Watershed Modeling System (WMS Software) Water Management System
WSPM	Weighted Spatial Probability Model.

1 Introduction

The Sinai Peninsula is located in the northeastern portion of Egypt and is bounded by longitudes 32°20′–34°52′E and latitudes 27°45′–31°10′N (Fig. 1). It occupies a part of the arid belt of northern Africa and southwest Asia (UNESCO, 1977). It occupies an area of about 61,000 km^2 or about 6% of Egypt's total area with a population of about 400,000, which is mainly bedouins (60%), and the rest are located in small cities such as El-Arish and Sharm El-Sheikh. The Peninsula has a triangular shape; its apex is to the south at Ras Mohammed (south of latitude 28°), whereas its base is to the north extending along the Mediterranean Coast between Port Said and Rafah for about 210 km (Figs. 1 and 2). Sinai is bounded in the eastern side by the Gulf of Aqaba and the International Border and in the west by the Gulf of Suez and Suez Canal. The peninsula has coasts extending for 900 km, including about 155 km along the eastern bank of the Suez Canal. Sinai's history is intertwined with many societies. Previous settlers include the ancient Egyptians, Nabataean's, Romans, Byzantines, and bedouins. Their experience in water harvesting and its exploitation can teach basic lessons to the new settlers of the late twenty-first century (Dames and Moore 1985).

Sinai suffers from an overwhelming water crisis. Runoff water harvesting (RWH) may be the optimum solution for such a problem (Elewa et al. 2012). The present work is dedicated to help the decision-makers and environmental planners by proposing appropriate locations and controlling systems for the RWH and the implementing runoff farming and rain-fed agriculture. This main objective could be performed by determining the promising areas for the RWH.

Remote sensing (RS), geographic information systems (GIS), and watershed modeling (WM) tools are useful in determining the potential locations for the RWH (Elewa et al. 2013; Rahman et al. 2014). Drought management in dry areas of Sinai will heavily depend on the particular planning in exploitation, investigation, and utilization of water resources for favoring the human requirements. Planning should depend on the drainage basins that intercept intermittently the flash floods, where effective methodologies and systematic information of the resources base are selected to measure, analyze, and formulate objectives of water resources development by the RWH (Elewa et al.

Fig. 1 ETM+ satellite image of Sinai Peninsula (Elewa et al. 2013)

2012). Accordingly, planning for maximizing the RWH, as an inherited historical technique, becomes an urgent need in order to cope with the human requirements and overcoming water scarcity problem. Maximizing the RWH will have its vital role in improving the groundwater recharging, raising water levels, and reducing its salinities to be suitable for the different uses. RWH could be efficient and may support the installment of new settlements in arid areas, with a direct impact on raising the quality of life of local inhabitants (Elewa and Qaddah 2011; Elewa et al. 2012, 2015, 2016; Yazar and Ali 2016). RWH is a well-known practice to improve water security and agricultural production (Paz-Kagan et al. 2017). Watershed management aims at enhancing the water availability in rain-fed areas through water conservation structures, which facilitate storage of water and recharge to groundwater by applying optimum

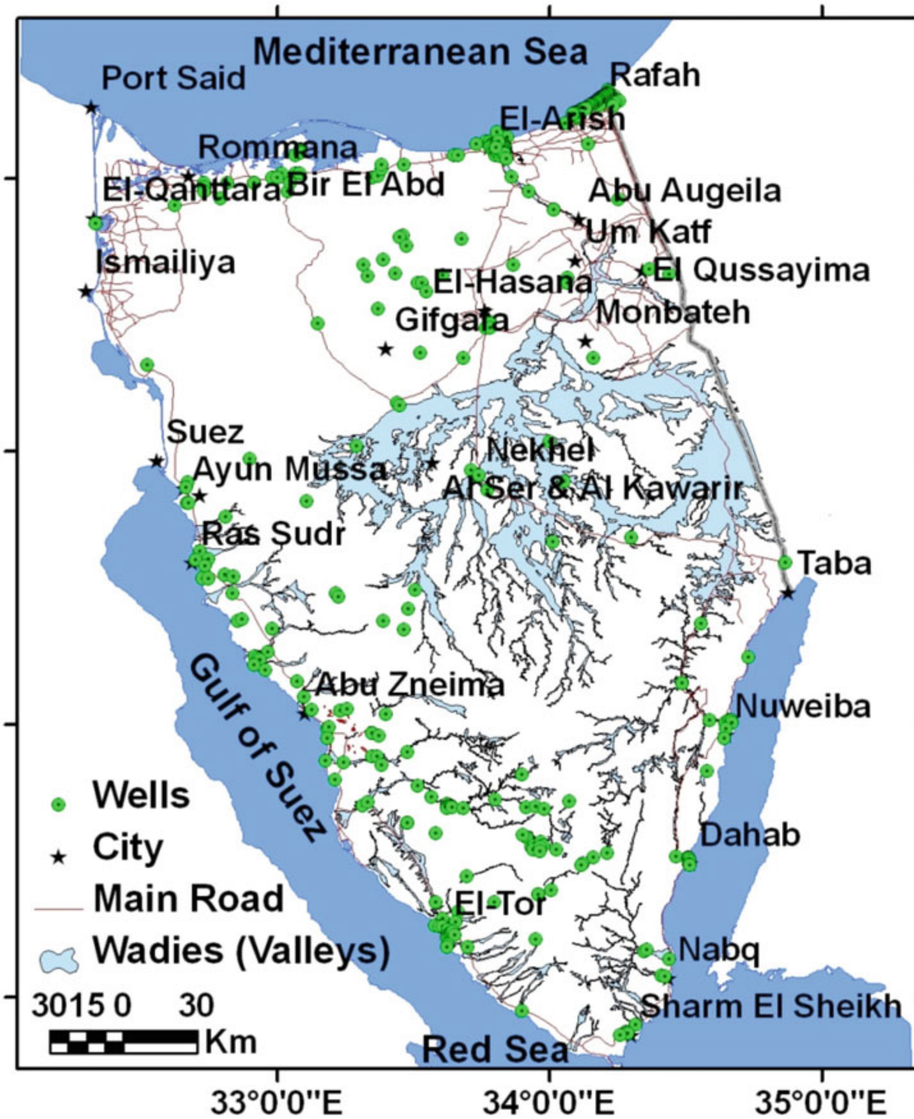

Fig. 2 The main physiographic features of Sinai Peninsula

RWH system (Vema et al. 2019). The present work involves an integrated framework of GIS, RS, and WM for determining optimum sites for RWH constructions in Dahab basin, south Sinai. Applications of RS, GIS, and statistical methods in extracting and analyzing the hydro-morphometric parameters of watersheds have a vital role in optimizing the evaluation of flash flood potentialities (Aher et al. 2014; Elewa et al. 2012, 2013, 2014, 2016). Weighted spatial probability modeling (WSPM) was used in the present context for determining the optimum sites for RWH in W. Dahab. The constructed model is based mainly on the most effective hydro-morphometric parameters of W. Dahab sub-watersheds. Wadi Dahab is considered a promising basin in southeastern Sinai, Egypt, where many tourist areas are located, which is very important for the Egyptian national income.

1.1 Site Description

Dahab watershed is located in the southeastern part of Sinai Peninsula and is bounded by longitudes 33°55′46.9″ and 34°31′28.8″ E and latitudes 28°22′43.4″ and 28°52′18.5″ N (Fig. 3). It occupies an area of about 2071.26 km^2.

1.2 Climate

Wadi Dahab area generally has an arid climate with quite significant rainfall intensity. Severe floods from Wadi Dahab Watershed could cause significant damage and loss of lives at the City of Dahab and along the main streams. Due to the meteorological conditions of South Sinai, flood events are sporadic, but severe. The affected areas include tourist locations, as well as residences of local inhabitants. Flash

Fig. 3 Wadi Dahab study area

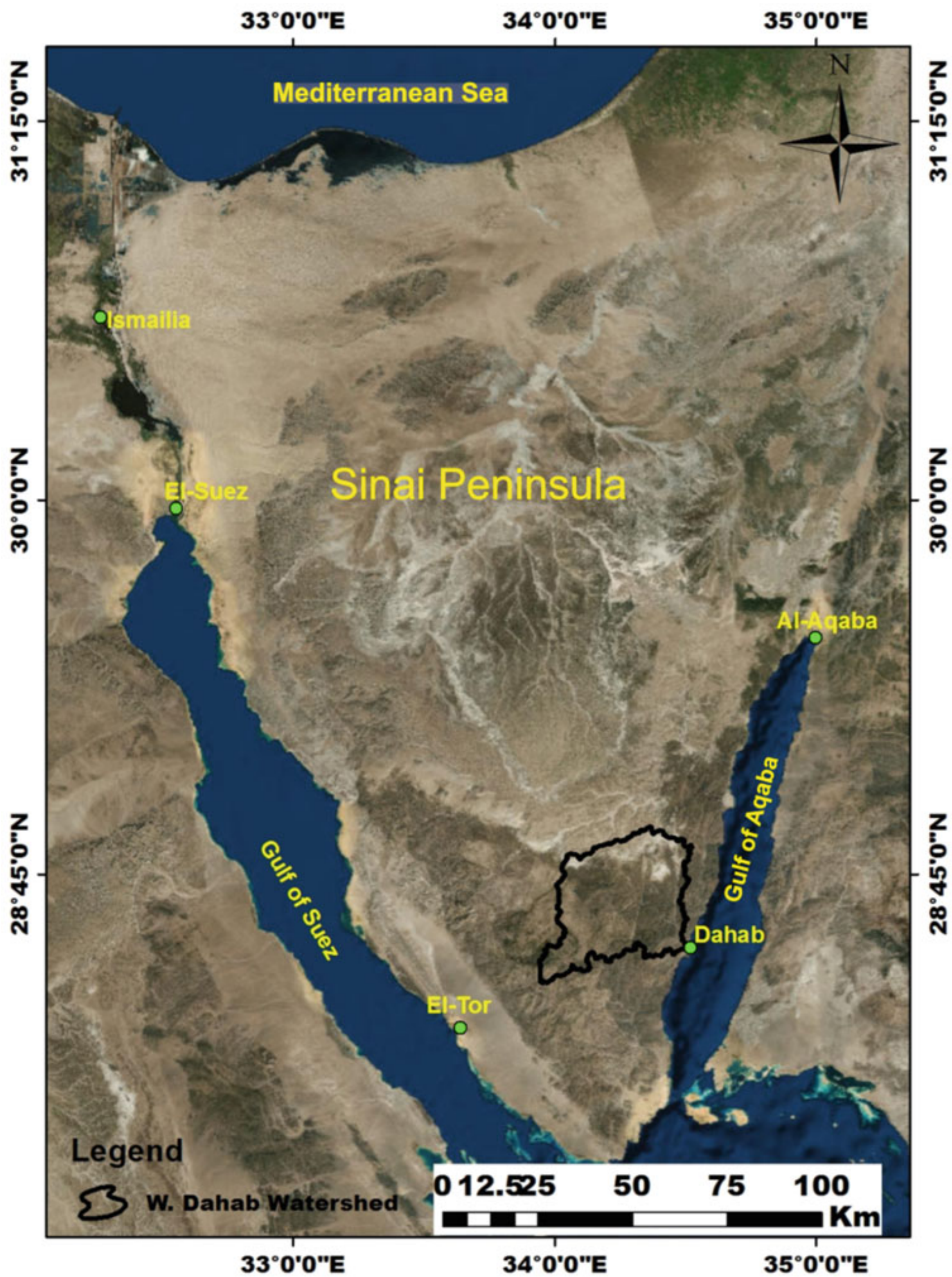

flood disaster is a major problem due to its diverse topography combined with meteorological and morphological conditions (Bisht et al. 2018). "The maximum intensity of rainfall, which has been recorded for a storm event of 24 h is 76 mm, which means that the area has received about 159 million m^3 with a return period of 100 years" (Omran 2013). Based on the climate conditions and the geology of the area, it could be concluded that about 50% of the precipitation is lost via evapotranspiration and infiltration, so that only half of the rainfall contributes to runoff. However, this is still enough to cause potential catastrophic effects on the infrastructure (Figs. 4 and 5).

1.3 Geological Conditions

Wadi Dahab is covered mainly with Cretaceous to Pre-Cambrian rocks. Sedimentary rocks of Cambrian to Cretaceous ages are located in the northern part of W. Dahab basin, while the rest of the basin is covered with pre-Cambrian rocks (igneous and metamorphic rocks), in addition to the recent wadi deposits, which cover the valley floors of the main streams (Said 1971) (Fig. 6). These deposits receive huge amounts of recharge from the fractured basement rocks, which receives the sporadic storms in winter. The topographic elevations range between 14 m and

Fig. 4 A photo showing the sabotage affecting the main road to Dahab City, which is caused by the rigorous flash floods of W. Dahab Watershed

about 2500 m (amsl), where the Wadi slope varies from gentle to very steep (Figs. 7 and 8).

Based on the lithological conditions, the groundwater-bearing formations are classified into the alluvial and fractured basement aquifer systems. Surface water from flash floods moves downward and laterally through the open fractures to recharge the alluvial deposits of the main valleys (El Rayes 1992). Thus, alluvial deposits of Wadi Dahab Watershed receive large amounts of recharge from the fractured basement rocks, which receives the sporadic storms in winter.

The structural elements, such as the deep-seated shear zones, tension fractures, and thrust faults act as conduits for groundwater recharge and movement (Shendi and Oada 1999). Rainwater, which is directly infiltrated to the highly jointed upper units is gradually transmitted into the fault zones and alluvial aquifers through the weakly jointed lower units. The intersections of fractures are good sites for the occurrence of groundwater and localization of water wells (El KiKi et al. 1992).

2 Materials and Methods

To accomplish the work objectives, the following tasks were performed which address the undertaken methods and techniques:

ASTER DEM (30-m spatial resolution), SPOT-4 satellite images (acquired on March 28, 2005) and topographic maps (1:50000 and 1:100000 scales) were used as essential primary data to build the GIS and performing the watershed modeling system (WMS 8.0©; AQUAVEO 2008) to determine the basin boundary, main sub-basins, and basin drainage net map. The stream orders were given for each stream according to Strahler method for stream ordering technique (Strahler 1964) using the ArcGIS 10.1©_ software platform.

The watershed hydrographic criteria derived from the WMS 8.0 software, which were used for the determination of the RWH optimum sites, include volume of annual flood (VAF), overland flow distance (OFD), maximum flow distance (MFD), basin infiltration number (IF), drainage density (DD), basin area (BA), basin slope (BS), and basin length (BL). These layers were used as multi-decision support criteria for conducting a weighted spatial probability model (WSPM) inside the GIS. The eight layers were used in raster

Fig. 5 A photo showing the destroyed main road to W. Dahab Watershed

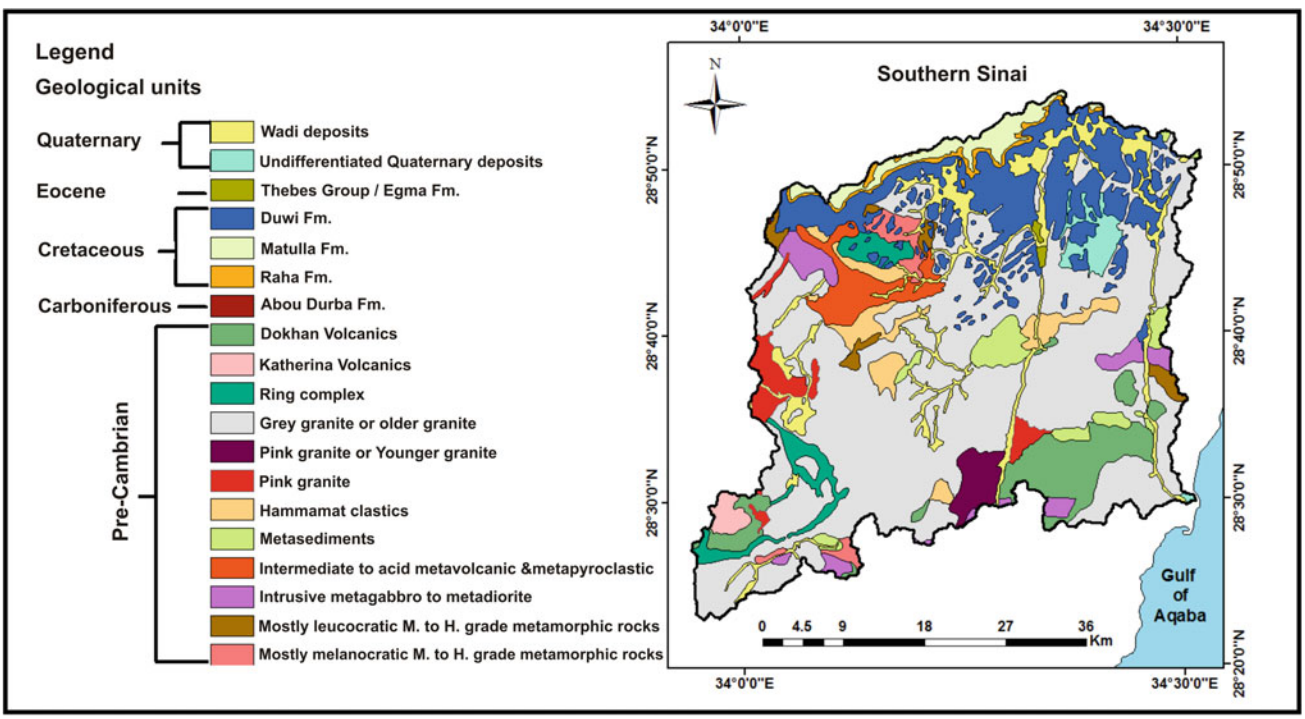

Fig. 6 Geological map of W. Dahab Watershed (simplified after CONOCO 1987)

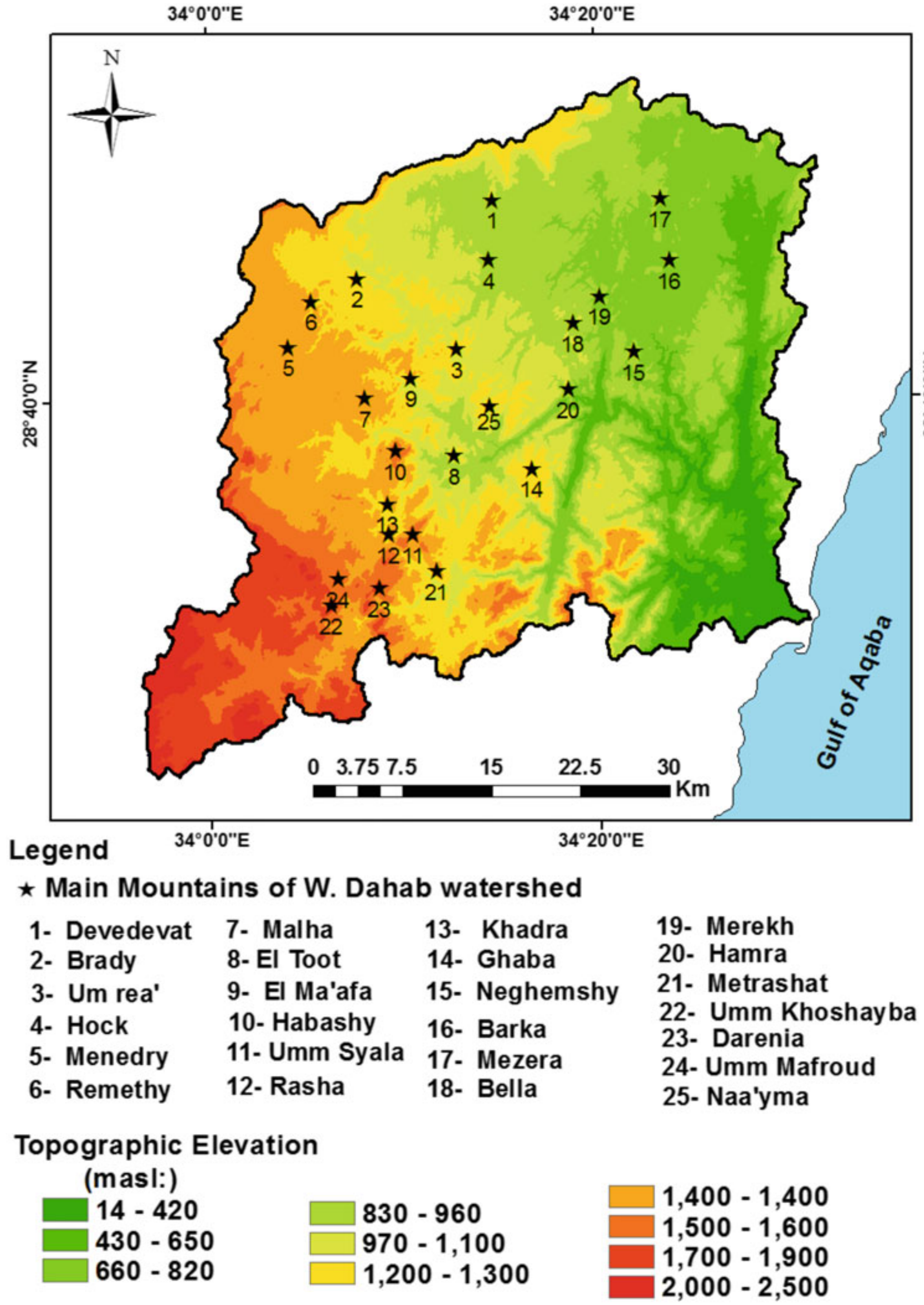

Fig. 7 Orographic features and topographic elevations of W. Dahab Watershed (based on ASTER DEM of 30 m resolution)

format and reclassified by the "Spatial Analyst tool" of the ArcGIS 10.1© software. Definite ranks and weights were given to each layer, depending on its contribution degree for the RWH and relation to the other parameters. WSPM was run three times for three scenarios; weights assigned by the equal weight to criteria (scenario I), weights assigned according to authors' experience (scenario II) and weights justified by sensitivity analysis (scenario III). The first scenario supposes equal weights for all thematic layers, whereas the second scenario involves the authors' knowledge to evaluate each criterion weight and/or also based on the experience added from the similar works (i.e., Javed et al. 2009; Montgomery and Dietrich 1989; Elewa and Qaddah 2011; Elewa et al. 2012, 2014, 2015, 2016). The third scenario is assigned according to the sensitivity analysis method (Van Griensven et al. 2006), which focuses on the impact of each parameter on the model output.

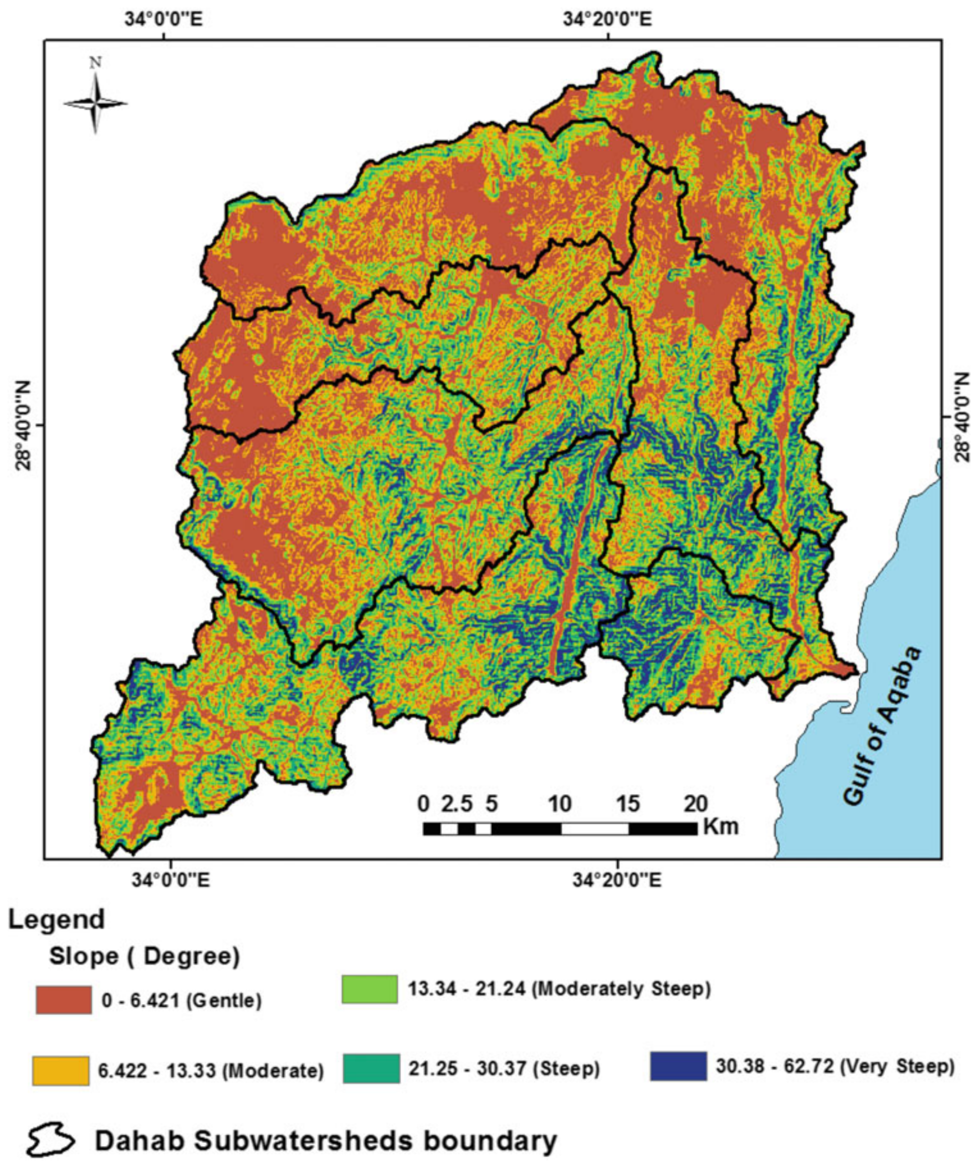

Fig. 8 Slope map of W. Dahab Watershed (based on 30 m resolution ASTER DEM)

The volume of the annual flood is calculated according to Finkel method (Finkel 1979), which was simulated by the WMS 8.0© software platform. Finkel (1979) used his method for the Araba Valley, which has similar climate conditions to Sinai Peninsula. It is a simple graphical method for determining the probability and frequency of occurrence of seasonal or yearly rainfall.

Finkel method (Finkel 1979) uses the following factors (Eqs. 1 and 2):

1. Peak flood flow (Q_{max})

$$Q_{\max} = K_1 A^{0.67} \quad (1)$$

where Q_{max} = Peak flood flows, in m^3/s.

2. Volume of the annual flood (v) in 1000 cubic meters

$$V = K_2 A^{0.67} \quad (2)$$

where A is basin area of the basin in km^2, and K_1 and K_2 are constants depending on the probability of occurrence

The overall flowchart of the methodology is given in Fig. 9.

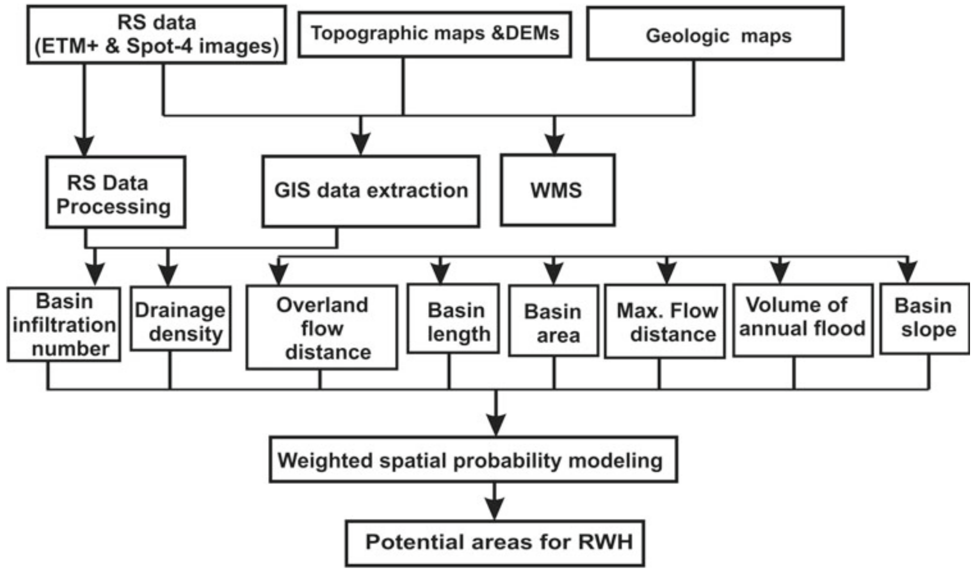

Fig. 9 Flowchart of methodology

3 Results of Watershed Modeling and Discussions

3.1 Generalities

Wadi Dahab Watershed consists of seven sub-watersheds (Fig. 10) and attains the 7th stream order (Fig. 11).

The following is a short description for W. Dahab sub-watersheds:

– **El-Ghaaib Sub-watershed**

This sub-watershed occupies about 297.9 km^2 with a trunk stream of the 4th order (Fig. 12). The wadi drains from the northern part of Baraka Mountain (800 masl) and Mezera Mountain (650 masl) (Fig. 7). The MFD of the watershed is 54.42 km with varying slopes from the gentle at the northern parts to the very steep in the southeastern side (Fig. 8). The average VAF resulting from W. El-Ghaaib is about 1,204,686.81 m^3 with a Q_{max} of 71.83 m^3/s occurring in an average flood duration of 16.77 h (Table 1).

– **Wadi Ganah Sub-watershed**

This sub-watershed is located at the northwestern part of W. Dahab Watershed and has the 5th order (Figs. 10 and 13). It occupies about 282.45 km^2. It drains from the Devedevat Mountain (420 m masl), Brady Mountain (1400 masl), and Remethy Mountain (1600 masl) (Fig. 7). The received VAF is about 1,162,453.75 m^3 with a Q_{max} of 69.31 m^3/s occurring in an average flood duration of 16.77 h (Table 1). The MFD is about 43.34 km. It is characterized by the gentle to moderately steep slopes in most parts of the sub-watershed (Fig. 8).

– **Wadi Saal Sub-watershed**

Wadi Saal sub-watershed occurs at the northwestern part of W. Dahab Watershed and occupies an area of about 242.56 km^2 (Fig. 10). The trunk channel has the 5th order, whereas the basin length attains about 34.19 km (Fig. 14). Wadi Saal drains mainly from Menedry and Malha Mountains of (1400 masl) (Fig. 7). The average VAF is 1,049,733.36 m^3 with a Q_{max} of 62.59 m^3/s within an average flood storm of 16.77 h (Table 1).

– **Wadi Zoghra Sub-watershed**

Wadi Zoghra is representing one of the largest sub-watersheds of W. Dahab among all W. Dahab sub-watersheds, where it encounters an area of about 415.99 km^2 (Fig. 10). Its trunk channel has the 5th order (Fig. 15). The MFD of the watershed is about 44.47 km. The VAF of W. Zoghra sub-watershed is about 1,506,716.76 m^3 with a Q_{max} of 89.83 within a flood storm of 16.77 h (Table 1).

– **Wadi Khoshaib Sub-watershed**

Wadi Khoshaib is the smallest sub-watershed of W. Dahab Watershed, where it encounters an area of about 108.57 Km^2 (Fig. 10). Its trunk channel has the 4th order (Fig. 16). It is characterized by a nearly circular shape and it is located in the southeastern side of W. Dahab Watershed close to W.

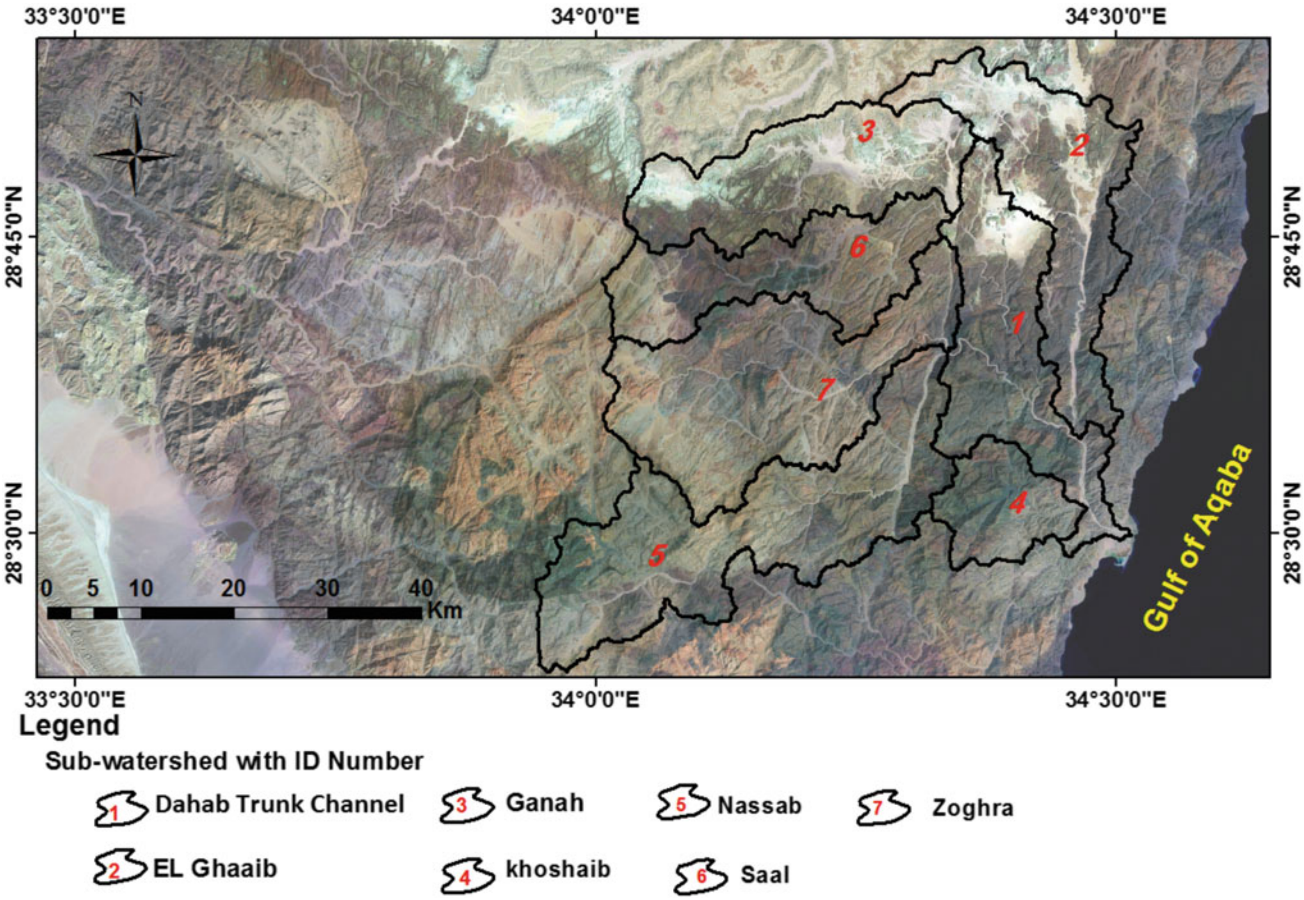

Fig. 10 A Spot-4 satellite image showing W. Dahab sub-watersheds

Fig. 11 A Spot-4 for W. Dahab watershed showing its stream orders

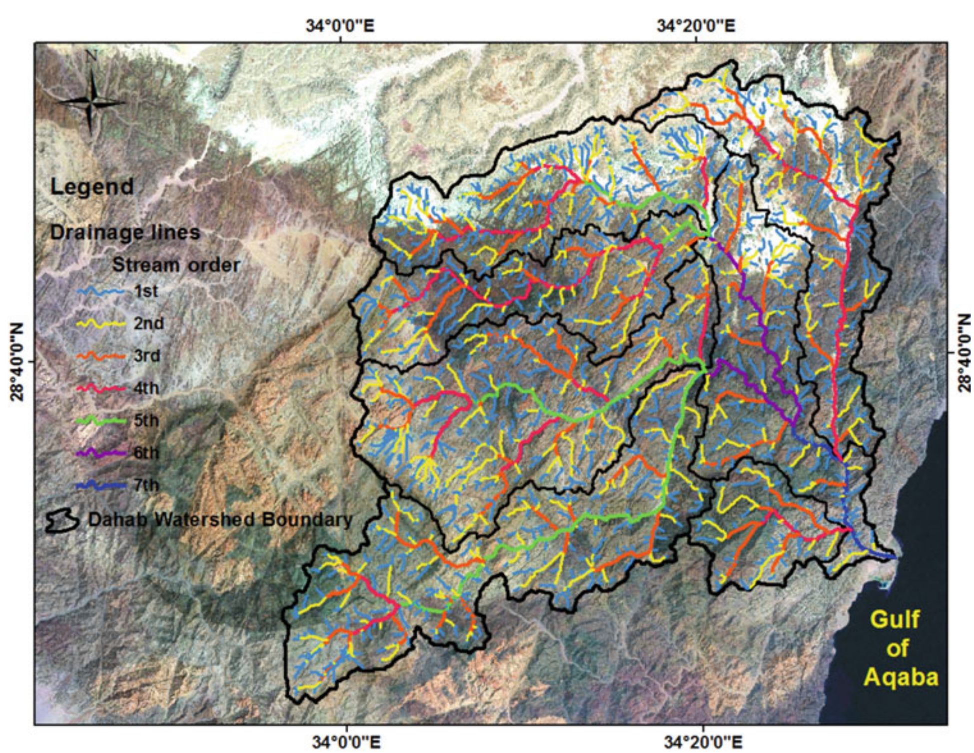

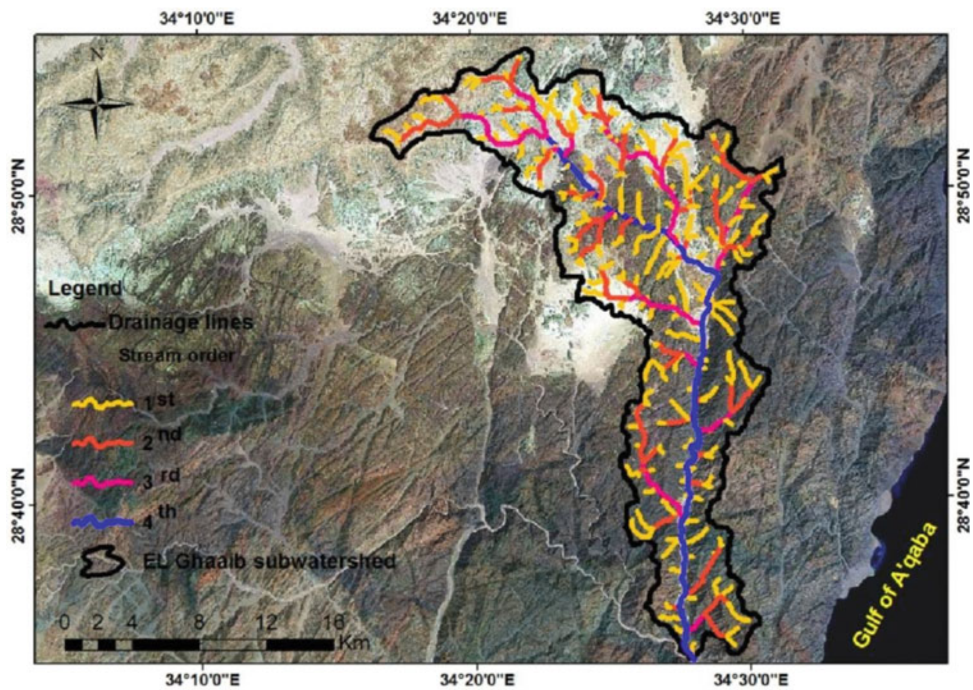

Fig. 12 A Spot-4 satellite image showing the location of W. El-Ghaaib sub-watershed

Table 1 WMS 8.0© software hydrographical output criteria used for demarcating the watersheds characteristics of W. Dahab Watershed

Basin ID	Sub-watershed	Average volume of annual flood (m^3)	Peak flood flow (Q_{max}) (m^3/s)	Overland flow distance (km)	Max. flow distance (km)	Basin infiltration no.	Drainage density (km^{-1})	Basin area (km^2)	Basin Slope (m/m)	Basin length (km)
W. Dahab Sub-Watersheds										
1	Dahab (Trunk Channel)	1,153,707.82	68.79	19.92	52.19	0.77	0.75	279.28	0.27	39.84
2	El-Ghaaib	1,204,686.81	71.83	18.92	54.42	0.83	0.79	297.90	0.20	37.84
3	Ganah	1,162,453.75	69.31	15.48	43.34	0.97	0.88	282.45	0.12	30.96
4	Khoshaib	612,592.39	36.52	7.37	19.63	0.59	0.58	108.57	0.37	14.74
5	Nassab	1,575,219.43	93.92	24.18	61.14	0.80	0.75	444.53	0.29	48.35
6	Saal	1,049,733.36	62.59	17.09	45.85	0.79	0.76	242.56	0.16	34.19
7	Zoghra	1,506,716.77	89.83	16.54	44.47	0.79	0.78	415.9	0.22	33.08
Average flood duration (h)	16.7									

Dahab Trunk Channel (Fig. 10). The MFD of the watershed is 19.631 km. It receives an average VAF of 612,592.39 m^3 with a Q_{max} of 36.52 m^3/s within a flood storm of 16.77 h (Table 1).

– Wadi Nassab Sub-watershed

Wadi Nassab sub-watershed is located in the southwestern part of W. Dahab Watershed with an area of 444.53 km^2 (Fig. 10) (Table 1). Its trunk channel has the 5th order (Fig. 17). It is characterized by an elongated shape, where torrents stem from the high mountains such as Umm Khoshayba (1800 masl), Umm Mafroud (1600 masl), and Darenia (1800 masl) (Fig. 7). It has a BL of about 48.35 km with an average OFD of 24.18 km, and MFD of 61.14 km. It receives an average VAF of about 1,575,219.43 m^3 with a Q_{max} of 93.92 m^3/s occurring within a flood storm of 16.77 h (Table 1).

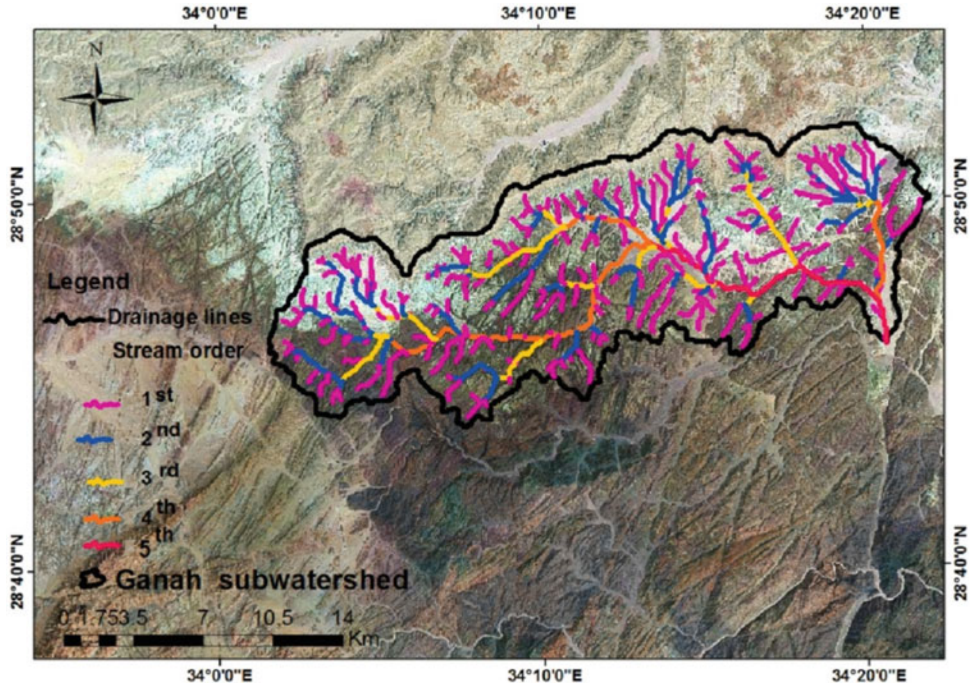

Fig. 13 A Spot 4-satellite image showing the location of W. Ganah sub-watershed

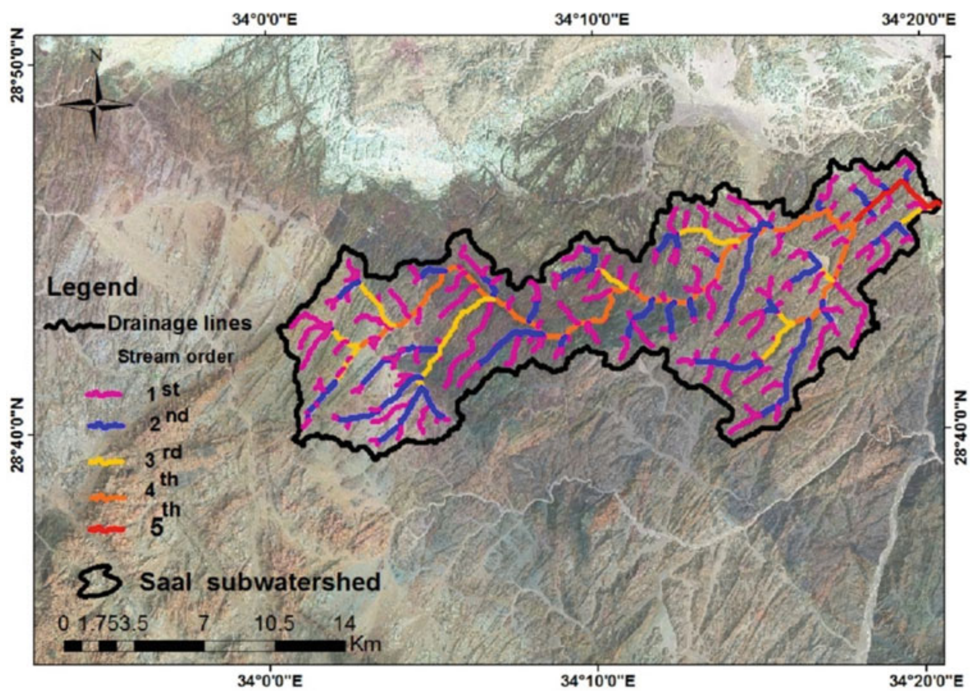

Fig. 14 A Spot-4 satellite image showing the location of W. Saal sub-watershed

– **Dahab Trunk Channel Sub-watershed**:

The Trunk Channel of W. Dahab Watershed debouches to the Gulf of Aqaba and occupies an area of about 279.28 km^2, with a trunk stream of the 5th order (Fig. 18) (Table 1). It originates from the northern parts of Dahab watershed to the outlet of the Wadi in the eastern side. It is characterized by varying slopes from gentle to very steep (Fig. 8). It has a BL of 39.8 km and a basin relief of 1.44 km. Average VAF is about 1,153,707.82 m^3 with a Q_{max} of 68.79 m^3/s occurring within a flood storm of 16.77 h. The MFD is 52.19 km and the average OFD is 19.92 km (Table 1).

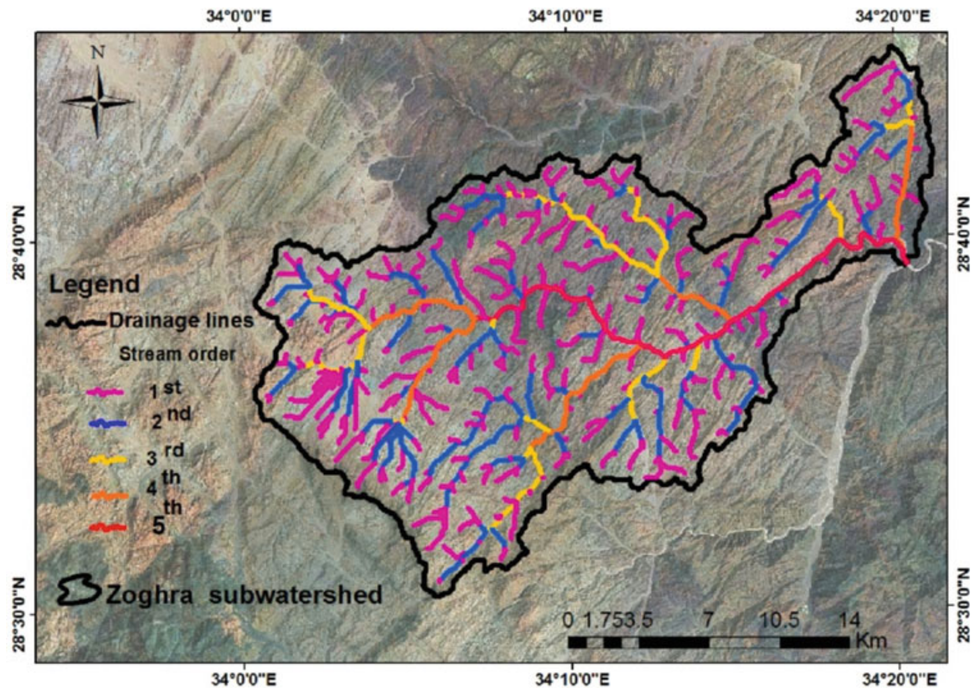

Fig. 15 A Spot-4 satellite image showing the location of W. Zoghra sub-watershed

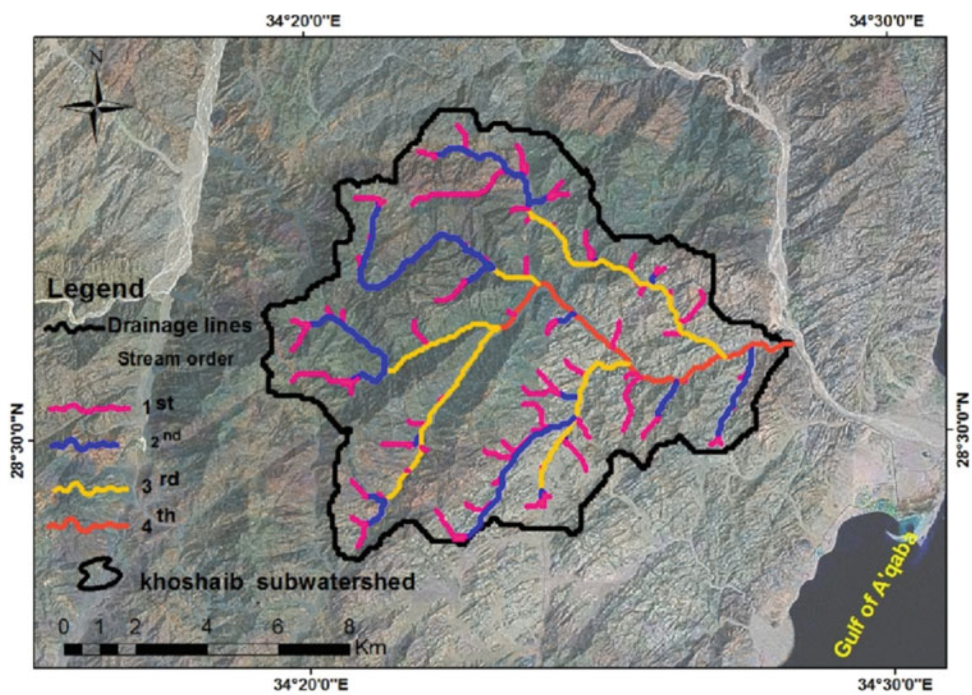

Fig. 16 A Spot-4 satellite image showing the location of W. Khoshaib sub-watershed

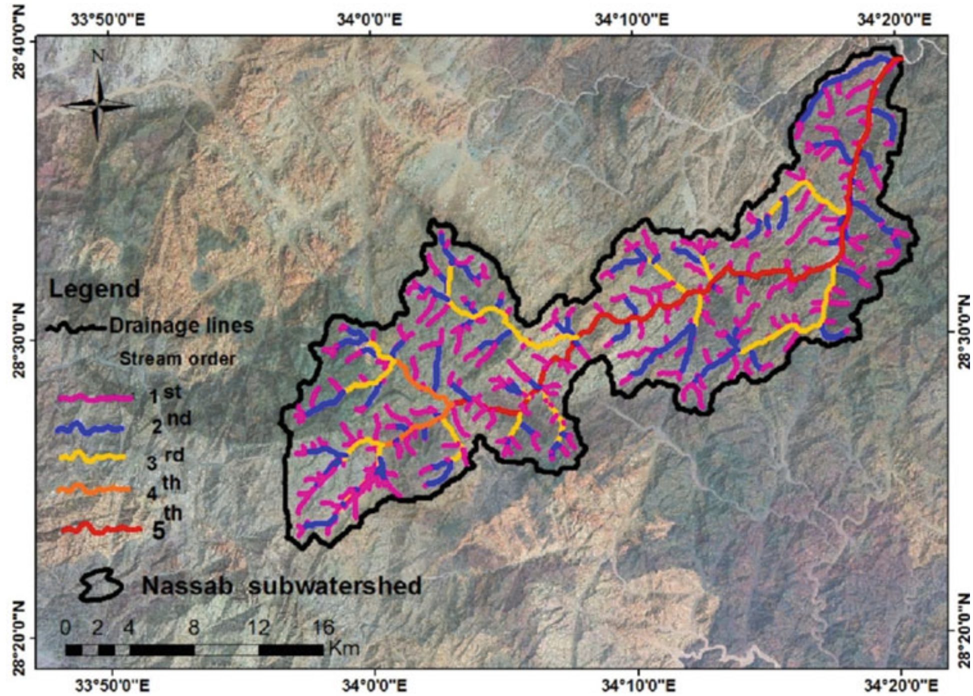

Fig. 17 A Spot-4 satellite image showing the location of W. Nassab sub-watershed

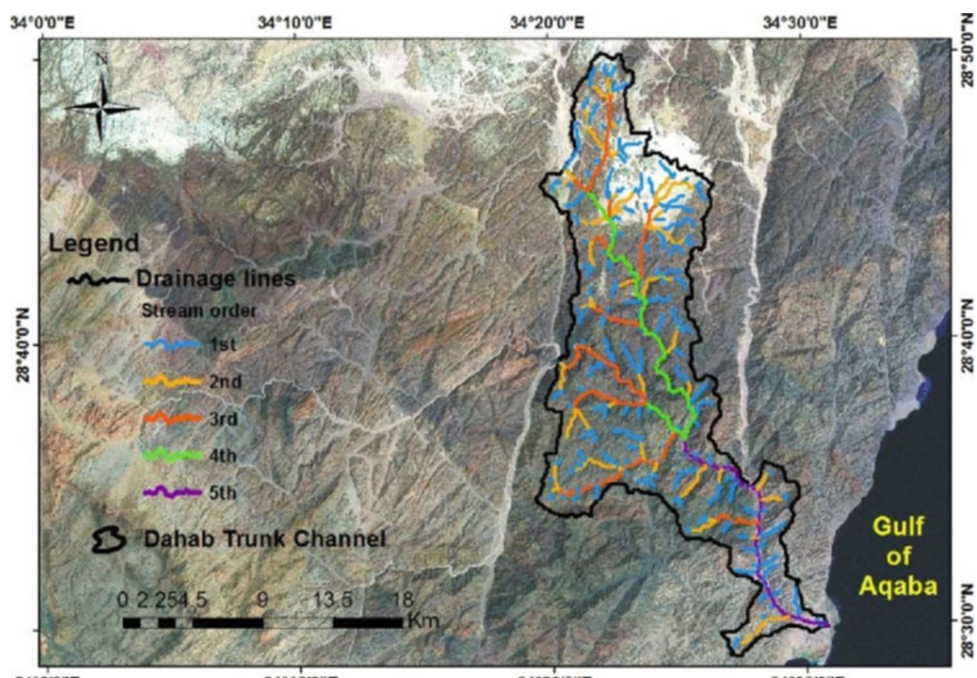

Fig. 18 A Spot-4 satellite image showing the location of W. Dahab Trunk channel sub-watershed

Table 2 Ranges of input criteria used for the WSPM of W. Dahab Watershed

Watershed RWH Criteria	Very high	High	Moderate	Low	Very Low
VAF (m^3)	>1,258,631.84	1,143,430.48–1,258,631.84	1,010,774.36–1,143,430.48	804,808.28–1,010,774.36	<804,808.28
OFD (km)	>20.80	18.00–20.70	15.10–17.90	11.30–15.00	<11.20
MFD (km)	>53.30	47.90–53.20	40.90–47.80	31.00–40.80	<30.90
IF	>0.89	0.83–0.89	0.76–0.83	0.68–0.76	<0.68
DD (km^{-1})	>0.81	0.76–0.81	0.71–0.76	0.65–0.71	<0.65
BA (km^2)	>385	321–384	263–320	192–262	<191
BS (m/m)	>0.32	0.27–0.32	0.22–0.27	0.17–0.22	< 0.17
BL (km)	>41.60	35.90–41.50	30.00–35.80	22.40–29.90	<22.40

3.2 Criteria of RWH Potentiality Determination in Wadi Dahab Watershed

The RWH potentiality of W. Dahab was determined by spatially integrating eight thematic layers, which represent the most decisive basin hydrographic and hydro-morphometric parameters.

These thematic layers, which represent the WSPM model inputs, include Average OFD, average VAF, BS, DD, BL, BA, IF, and the MFD (Table 1). The following is a short description of these themes for W. Dahab Watershed:

– **Average Overland Flow Distance (OFD)**

The OFD within the basin is computed by averaging the overland flow distance; traveled from the centroid of each triangle to the nearest stream. Most of W. Dahab Watershed is represented by the moderate and high classes for the average OFD (15.10–17.90 km and 18.00–20.70 km, respectively) (Table 2), which covers almost the areas of El-Ghaaib, Ganah, Saal, and W. Dahab Trunk Channel sub-watersheds, and covers also some parts of Zoghra and Nassab sub-watersheds (Fig. 19). However, the variation in relief and slopes determines where the overland is effective and generated.

The thematic layer of the OFD indicates a pronounced decrease in value on the southeastern side of W. Dahab near its outlet at the Gulf El-Aqaba, where low (11.3–15.00 km) and very low class (<11.20 km) occur and cover some areas of Nassab, Dahab Trunk Channel, and Khoshaib sub-watersheds. Very high OFD class (>20.80 km) occurs in southwestern parts of W. Dahab and covers some areas of Nassab and Zoghra sub-watersheds (Fig. 19).

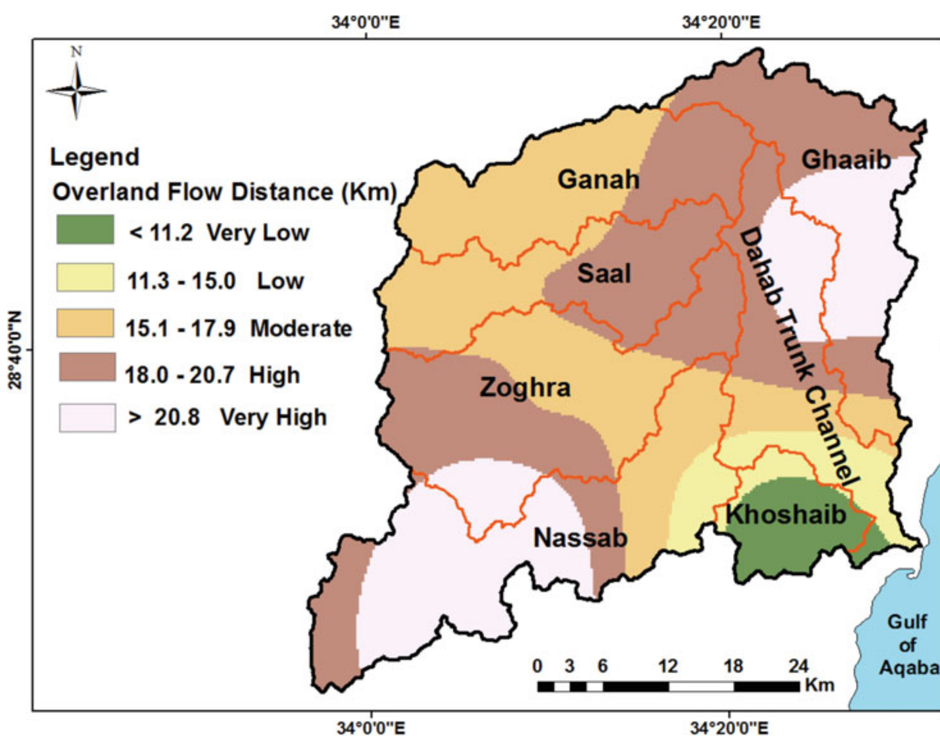

Fig. 19 The OFD thematic layer used in the WSPM of W. Dahab Watershed

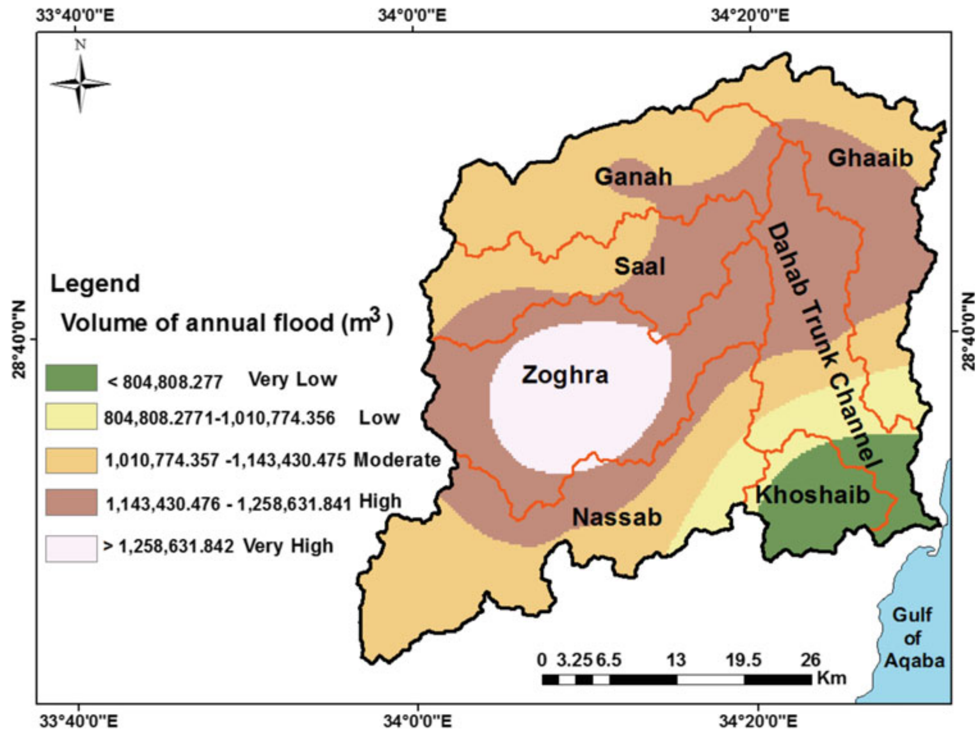

Fig. 20 VAF thematic layer used in the WSPM of W. Dahab Watershed

– **Average Volume of Annual Flood (VAF)**

The availability of a pronounced VAF in a drainage basin is one of the most significant parameters for the success of the RWH (Elewa and Qaddah 2011). W. Dahab was classified into five classes relative to its potential for the VAF generation, which was calculated according to Finkel's method. Figure 20 shows that almost the central parts of W. Dahab are classified as of high-very high classes for the VAF generation (>1,143,430.48 m^3), which represent the whole area of Zoghra and some areas of Nassab, Saal, Ganah, Ghaaib, and Dahab Trunk Channel sub-watersheds. Almost the remaining areas of these sub-watersheds were classified as of moderate class (1,010,774.36–1,143,430.48 m^3). Low-very low classes (<804,808.28 m^3) represent the lower reaches of Nassab, Khoshaib, and Dahab Trunk Channel sub-watersheds.

– **Basin Slope (BS)**

The BS map was generated from the ASTER DEM of 30-m resolution. The slope map was merged with the basin map to create the slope attributes of each drainage basin. Five BS classes were generated (Fig. 21). This map indicates a linear increase in slope values from the north, northwest, and southeast toward the eastern side at the outlet of W. Dahab Watershed (Fig. 21, Tables 1 and 2). The very steep BS is represented by Khoshaib and some areas of Dahab Trunk Channel sub-watersheds. However, this variation in BS is attributed to the general watershed slope and local geological and structural setting of W. Dahab Watershed.

– **Drainage Denisty (DD)**

W. Dahab Watershed was classified according to the DD into five classes (Fig. 22; Table 2). The thematic layer of the DD indicates a linear decrease in DD values from the upstream northern and western sides toward the southeastern side at the outlet of W. Dahab Watershed (Fig. 22). However, this variation in the DD values is mainly attributed to the lithological nature of exposed geological units, which are represented by the sedimentary rock units of Quaternary age (wadi and undifferentiated deposits), fractured limestones of Eocene Thebes Group, Duwi clay stone, siltstone with interbeds of phosphate-bearing units, Matulla Fm of fluvial and cross-bedded sandstone and varicolored glauconitic shale, Raha Fm of fine-grained glauconitic and pyritic sandstone with grey calcareous shale of Late Cretaceous (Said, 1962, 1990; CONOCO 1987). These rock units are characterized by soft surface soils with low vertical permeability that causes a noticeable increase in the DD values in these parts of the watershed (Figs. 6 and 22) (i.e., >0.814 km^{-1} and 0.764–0.813 km^{-1} for the very high and high DD classes, respectively). In contrary to the southeastern and southwestern parts of the watershed, which are covered by moderately fractured grey or older granites or

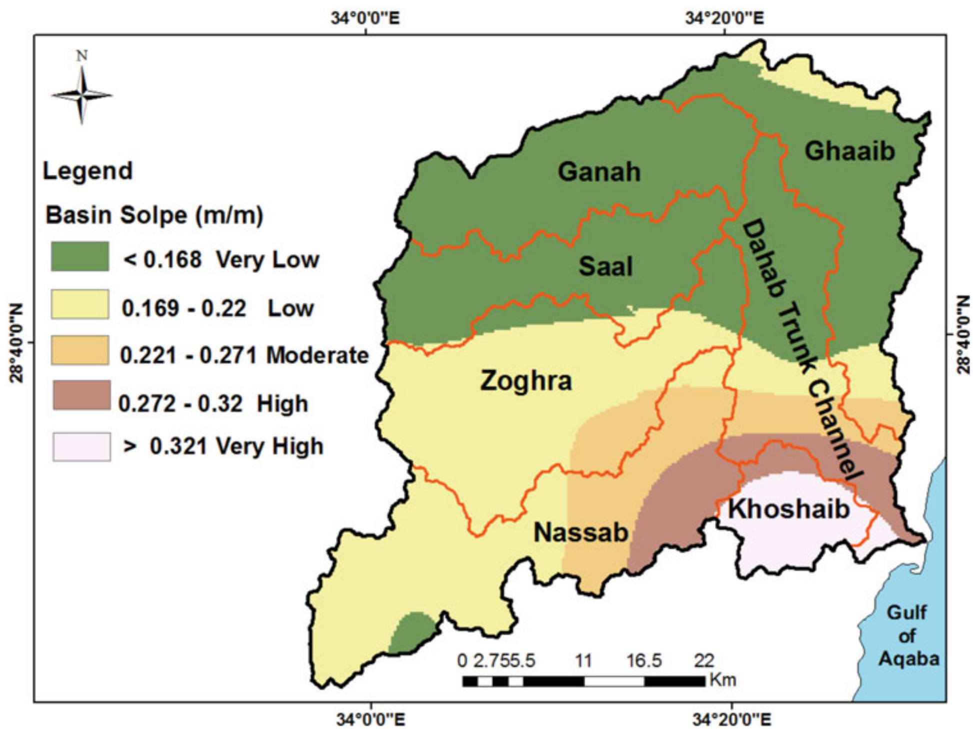

Fig. 21 The BS thematic layer used in the WSPM of W. Dahab Watershed

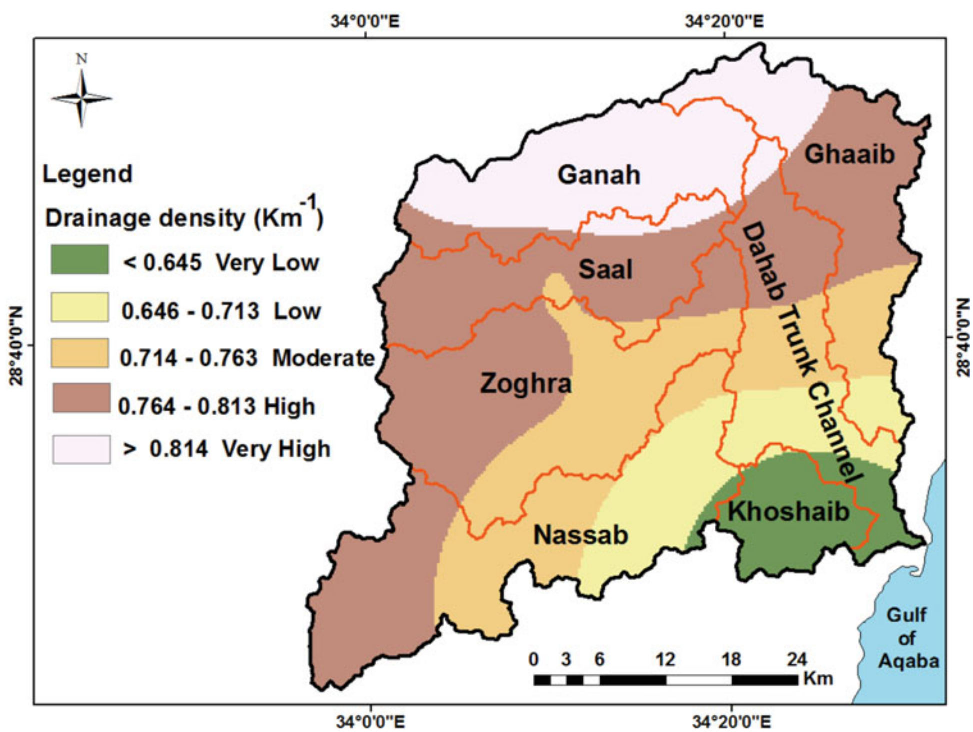

Fig. 22 The DD thematic layer used in the WSPM of W. Dahab Watershed

the highly metamorphosed rocks, which despite their very negligible rock porosity are having a reasonable vertical fracture permeability that causes the DD values to be low and very low (i.e., <0.65 km^{-1}). However, in consolidated sedimentary rocks and igneous and metamorphic rocks, fracture flow will almost invariably occur and hence a wide range of values of hydraulic conductivity can occur for any one lithology, depending on both the degree of fracturing and the size of the fractures (Lewis et al. 2006), which is clear in the southwestern areas of the watershed, where highly metamorphosed melanocratic rock of very low permeability occur (Figs. 6 and 22). The previously discussed facts that stand behind the reasons of spatial variation in the DD are also dramatically reinforced by the map of IF, where high-very high IF values are encountered in the sedimentary rock territories reflecting the low vertical rock permeability, hence their higher DD values (Fig. 22).

– **Basin Length (BL)**

The thematic layer of BL for W. Dahab Watershed was classified into five classes, where the more compacted basins, like those occurred in southeastern parts of W. Dahab Watershed represent the very low class (<22.30 km), which was occupied by W. Khoshaib sub-watershed (Fig. 23). This class was followed by the low class (22.4–29.9 km) that represents some areas in the downstream of Nassab and Dahab Trunk Channel sub-watersheds. The northeastern and central parts of W. Dahab Watershed were classified as of moderate class (30–35.8 km), which was represented by some parts of El-Ghaaib, Zoghra, Ganah and Dahab Trunk Channel and most areas of Saal sub-watersheds. The high (35.9–41.5 km) and very high (>41.6 km) classes of the BL were represented by some areas in the eastern and southwestern parts of W. Dahab Watershed, which were represented by the El-Ghaaib, Zoghra, Ganah, Saal, and Dahab Trunk Channel, Zoghra and Nassab sub-watersheds.

– **Basin Area (BA)**

Basin area has been identified as the most important of all "morphometric parameters controlling the catchment runoff pattern. This is because, the larger the size of the basin, the greater the amount of rain it intercepts and the higher the peak discharge that results" (Faniran and Ojo 1980). A thematic layer of BA with five classes was generated (Fig. 24). The very high (>385 km^2) and high (321–384 km^2). BA classes occur in the southwestern parts of the watershed, which are covering some areas of Zoghra and Nassab sub-watershed. Moderate class (263–320 km^2) (Table 2) represents the most area of W. Dahab in El-Ghaaib, Ganah, Saal, Zoghra, Nassab, and Dahab Trunk Channel sub-watersheds. Low class (192–262 km^2) is represented by the upstream parts of Saal and Ganah, and some parts are occurring at the southeast that is represented by El-Ghaaib, khoshaib, and Dahab Trunk Channel sub-watersheds. Very low BA class (<191 km^2) is represented by Khoshaib and outlet part of W. Dahab Trunk Channel sub-watersheds.

– **Basin Infiltration Number (IF)**

The IF map with five classes was produced to reveal the infiltration capabilities and their effect on the RWH capabilities of W. Dahab Watershed. The thematic IF layer indicates a linear decrease in IF values from the upstream northern–southwestern parts toward the southeastern downstream reaches of W. Dahab Watershed, indicating a

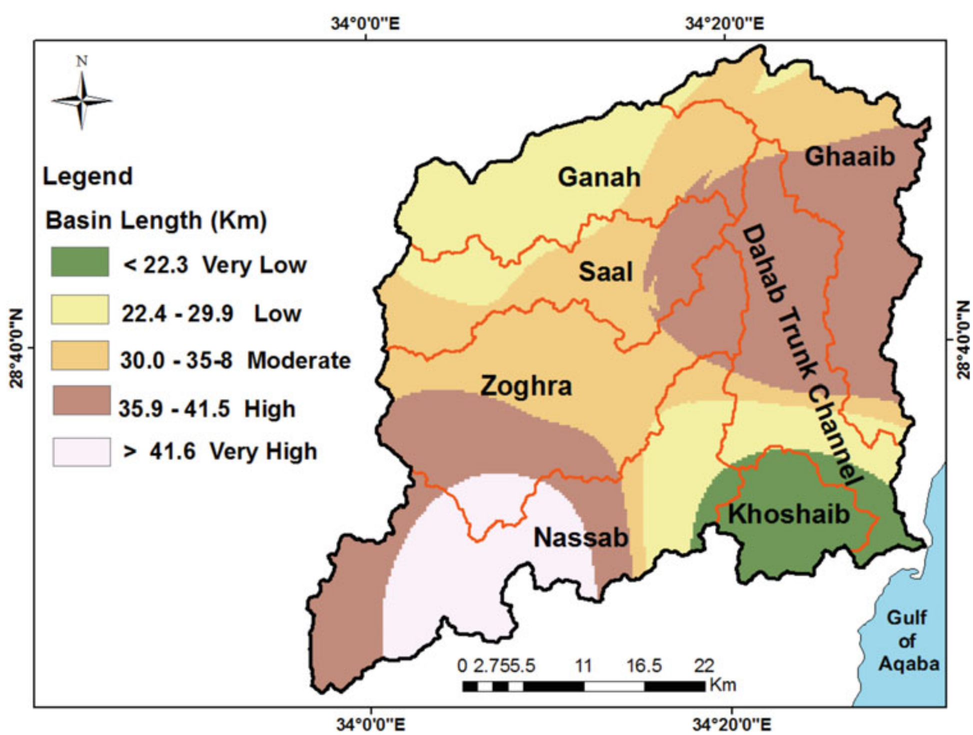

Fig. 23 The BL thematic layer used in the WSPM of W. Dahab Watershed

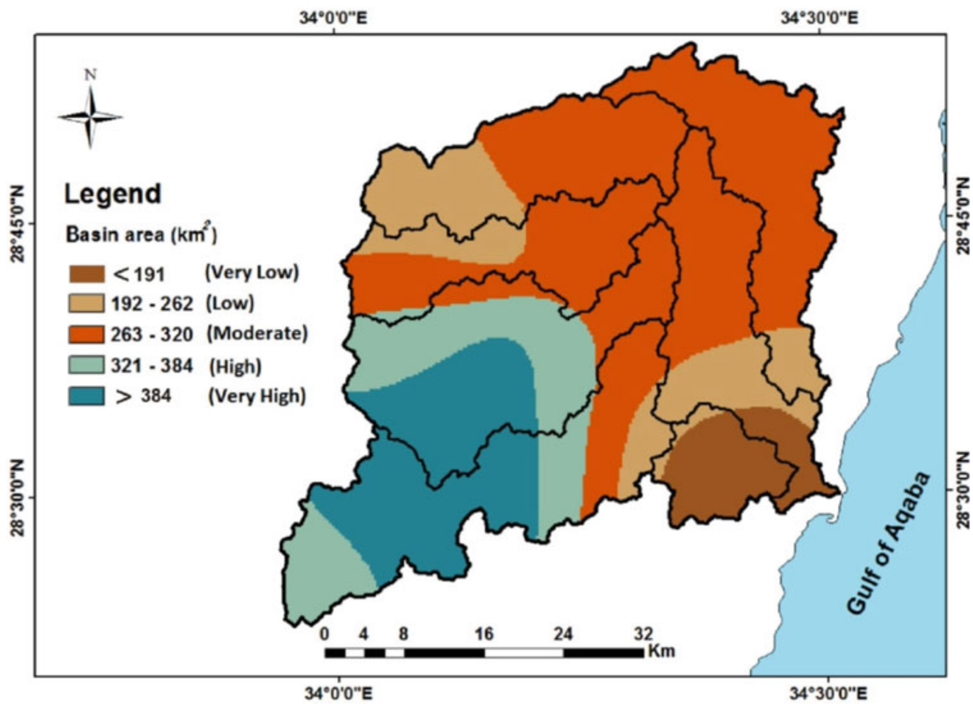

Fig. 24 The BA thematic layer used in the WSPM of W. Dahab Watershed

pronounced increase in infiltration capabilities in the same directions (Fig. 25). However, this variation in the IF has mainly attributed the facies change of different lithologic units exposed in the study area, as previously discussed. The IF classes are very high (>0.8939), high (0.8284–0.8938), moderate (0.763–0.8283), low (0.6792–0.7629), and very low (<0.6791) (Table 2; Fig. 25).

– **Maximum Flow Distance (MFD)**

The very low (<30.9 km) and low (31.0–40.8 km) MFD classes are represented by the southeastern parts of W. Dahab Watershed that cover the most areas of Khoshaib and some areas of Nassab, and Dahab Trunk Channel sub-watersheds (Fig. 26; Table 2). High (47.9–53.2 km) and

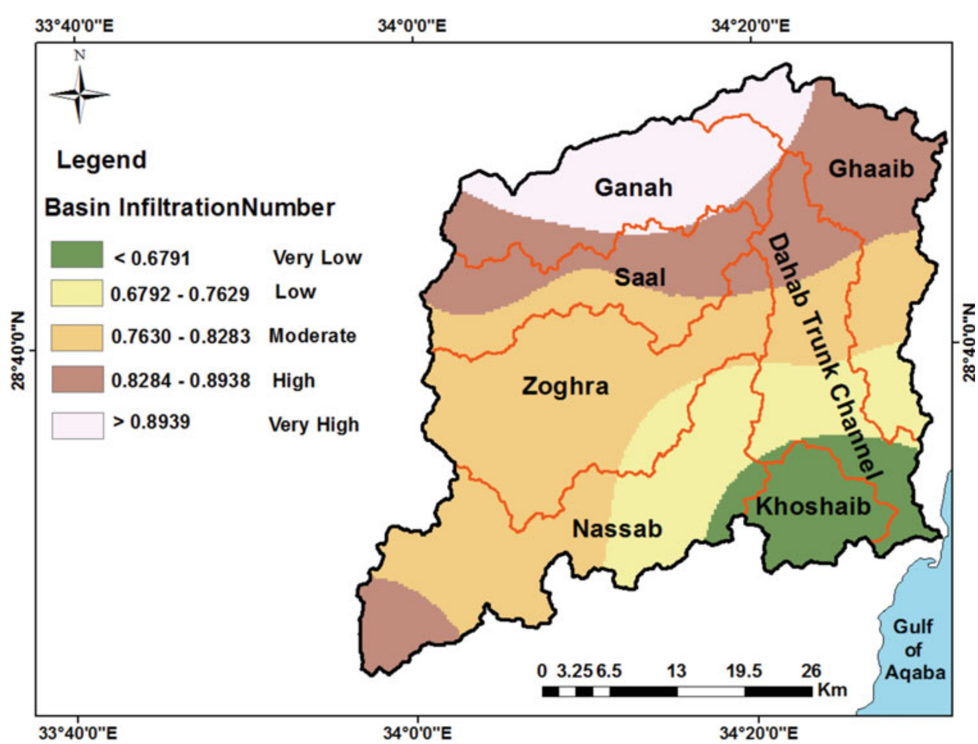

Fig. 25 The IF thematic layer used in the WSPM of W. Dahab Watershed

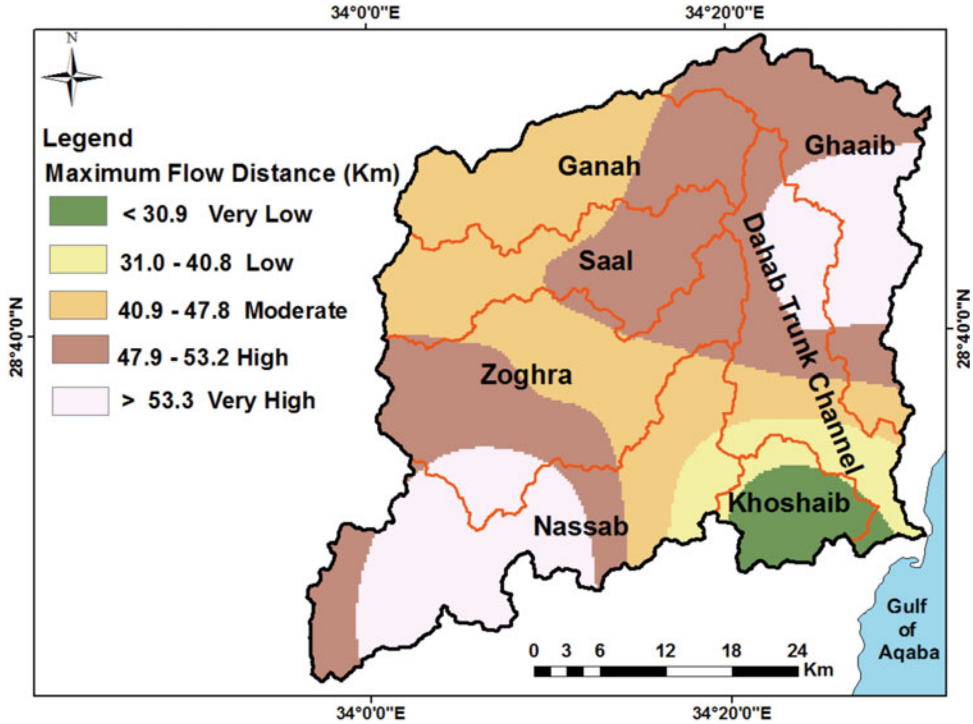

Fig. 26 The MFD thematic layer used in the WSPM of W. Dahab Watershed

very high (>53.3 km) MFD classes are represented in two localities; the first one occurs in the northeastern-eastern areas, which are occupied by some parts of El-Ghaaib, Ganah, Saal, Zoghra, and Dahab Trunk Channel sub-watersheds, whereas the second one is represented by the southwestern side, which is covered by some areas of Zoghra and Nassab sub-watersheds. The moderate MFD class (40.9–47.8 km) covers large areas of Ganah, Saal, Zoghra, Nassab, and Dahab Trunk Channel sub-watersheds.

3.3 Weighted Spatial Probability Modeling (WSPM) for Determining the RWH Potentialities of W. Dahab Watershed

The WSPM for W. Dahab Watershed was also run by the same previously discussed manner, where three scenarios were performed; i.e., equal weights to criteria, weights proposed by the authors, and weights justified by the sensitivity analysis.

– **WSPM's Scenario I (equal weights to criteria)**:

In this first WSPM's scenario, the previously discussed eight thematic criteria are proposed to have equal degrees of contribution in the potentiality mapping for RWH where the integrated criteria were given an equal weight of 12.5% with a summation of 100% for all data themes. The classes were categorized from I (very high potentiality) up to V (very low potentiality) in the RWH potentiality mapping (Table 3). Considering 100% for the maximum value of the rank, thus for the five classes; ranks will be classified as 100–80, 80–60, 60–40, 40–20, and 20–0%, respectively. Consequently, the average ranking for each class will be 0.90, 0.70, 0.50, 0.30, and 0.10% for classes from I to V, respectively (Table 3). The effectiveness degree (E) for each thematic layer was calculated by multiplying the criterion weight (W_c) with the criterion rank (R_c). For example, if the weight of VAF equals 12.5% and this is multiplied by the average rank of 90 (for a class I), the degree of effectiveness will be 11.25 (Eq. 3).

$$E = W_c \times R_f = 0.125 \times 90 = 11.25 \quad (3)$$

According to data manipulation method, the valuation of the effectiveness of each decision criterion provides a qualified analysis of the different thematic layers. A resulted WSPM map for RWH potentiality with five classes ranging from the very low to very high potentiality was obtained (Fig. 27).

The spatial distribution of these classes relative to the total study area is 3.82 (very low), 8.55 (low), 24.67 (moderate), 42.98 (high), and 19.96% (very high) for RWH potentiality mapping (Fig. 27; Table 4).

From this WSPM map, it could be concluded that the major area of W. Dahab is categorized as of high and very high potentiality for the RWH (i.e., 62.94% of total watershed area), especially in its northeastern, eastern, central, western, and southwestern parts of W. Dahab, the RWH is

Table 3 WSPM scenario I (equal weights to criteria), ranks and degree of effectiveness of themes used for the RWH potentiality mapping of W. Dahab Watershed

Thematic layer (criterion)	RWH potentiality class	Average rate (Rank) (R_c)	Weight (W_c)	Degree of effectiveness (E)
VAF	I (Very high) II (High) III (Moderate) IV (Low) V (Very low)	0.9 0.7 0.5 0.3 0.1	12.5	11.25 8.75 6.25 3.75 1.25
OFD	I (Very high) II (High) III (Moderate) IV (Low) V (Very low)	0.9 0.7 0.5 0.3 0.1	12.5	11.25 8.75 6.25 3.75 1.25
MFD	I (Very high) II (High) III (Moderate) IV (Low) V (Very low)	0.9 0.7 0.5 0.3 0.1	12.5	11.25 8.75 6.25 3.75 1.25
IF	I (Very high) II (High) III (Moderate) IV (Low) V (Very low)	0.9 0.7 0.5 0.3 0.1	12.5	11.25 8.75 6.25 3.75 1.25
DD	I (Very high) II (High) III (Moderate) IV (Low) V (Very low) V (Very low)	0.9 0.7 0.5 0.3 0.1	12.5	11.25 8.75 6.25 3.75 1.25
BA	I (Very high) II (High) III (Moderate) IV (Low) V (Very low)	0.9 0.7 0.5 0.3 0.1	12.5	11.25 8.75 6.25 3.75 1.25
BS	I (Very high) II (High) III (Moderate) IV (Low) V (Very low)	0.9 0.7 0.5 0.3 0.1	12.5	11.25 8.75 6.25 3.75 1.25
BL	I (Very high) II (High) III (Moderate) IV (Low) V (Very low)	0.9 0.7 0.5 0.3 0.1	12.5	11.25 8.75 6.25 3.75 1.25

noticeably decreasing to low and very low potentiality for the RWH (8.55 and 3.82% of the total watershed area, respectively) at the downstream reaches and some areas in the southwestern part of the watershed (Fig. 27; Table 4).

– **WSPM's Scenario II (weights proposed by the authors)**:

Based on the weights proposed by the authors, the eight thematic layers (WSPM criteria) were superposed by the ArcGIS 10.1© within the Spatial Analyst Model Builder to perform the WSPM by taking the new authors' proposed weights as OFD (17%), VAF (16%), BS (12%), DD (12%), BL (12%) MFD (10%), IF (10%), and BA (11%) (Table 5). The WSPM output map with five classes ranging from the very low to very high potentiality was obtained (Fig. 28). The spatial distributions of these classes relative to the total watershed area were 7.56 (very low), 14.13 (low), 21.35 (moderate), 42.53 (high), and 14.42% (very high) potentiality for the RWH (Fig. 28; Table 6). From the WSPM scenario II, it is clear that the high and very high potential classes for the RWH encompasses about 56.95% of the total watershed area, compared to 62.94% in scenario I. Furthermore, the same spatial distribution of RWH potentiality classes was established by the WSPM scenario II map (Fig. 28; Table 6).

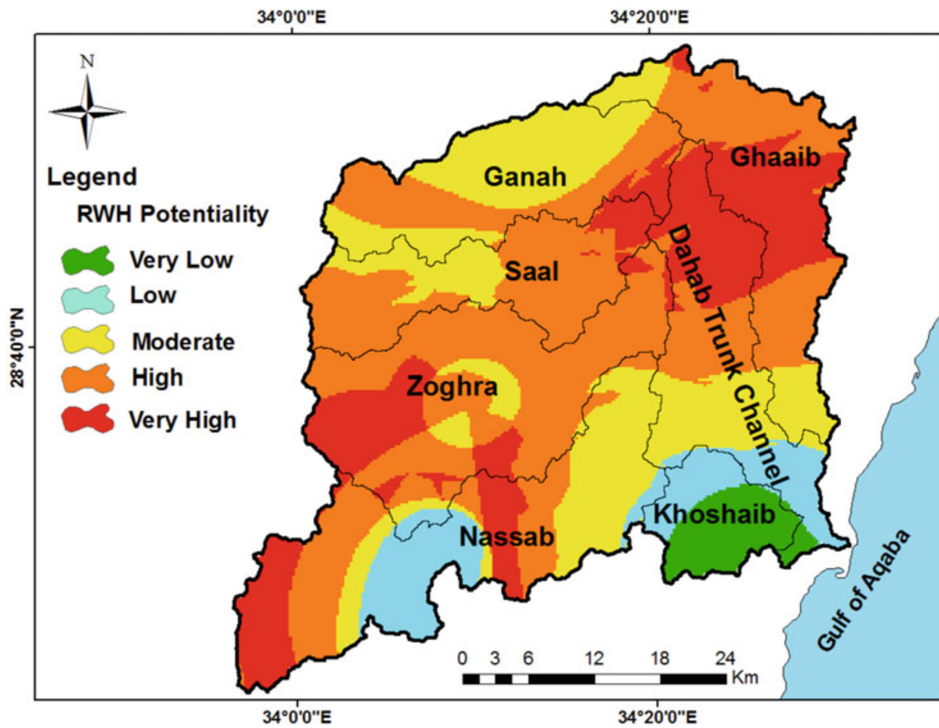

Fig. 27 WSPM's output map of Scenario I (equal weights to criteria) showing the RWH potentiality of W. Dahab Watershed

Table 4 Areas of RWH potentiality classes resulted from the WSPM Scenario I in W. Dahab Watershed

RWH potentiality map					
RWH potentiality class	Very low	Low	Moderate	High	Very high
Area (Km^2)	79.17	177.32	511.17	890.56	413.54
Area % relative to the total watershed area (Total watershed area: 2071.76 km^2) (%)	3.82	8.55	24.67	42.98	19.96

WSPM's Scenario III (Justified Weights by the Sensitivity Analysis) for the RWH Potentiality mapping of W. Dahab Watershed

In the third scenario, a sensitivity analysis (Van Griensven et al. 2006) was performed to justify the weights of the WSPM's criteria in order to attain a more justified or optimum RWH potential areas in W. Dahab.

However, to justify the WSPM's weights and results, we should take all the scenarios as different alternatives for assigning the criteria weights. The WSPM's sensitivity analysis for the determination of RWH potentiality was performed through the following steps:

- The first step (Scenario I) involves assuming that all the WSPM's eight thematic layers or criteria have the same magnitude of contribution or weights in the RWH potentiality mapping. In this scenario, all criteria were assigned an equal weight of 12.5% (equal effect) (Table 3).
- The second step was to determine the potentiality of RWH using the sensitivity analysis to justify the decisive criteria weights. The potentiality assessment of RWH sites involves the need to evaluate the consistency of the parameters used in the prioritization. A small perturbation in the decision weights may have an important influence on the rank ordering of the criteria, which afterward may ultimately modify the best choice and the model results. However, the uncertainties associated with MCDSS techniques are inevitable and the model outcomes are open to multiple types of uncertainty.

In each WSPM's running operation, seven parameters were kept with the same weights of 10%, while assigning only the remaining parameter with the residual 30% (Figs. 29 through 36) (Figs. 30, 31, 32, 33, 34, and 35).

The previously discussed WSPM's running practice is essential to apply the variance-based global sensitivity analysis (GSA) or what is called the analysis of variance (ANOVA), which subdivides the variability and apportions it to the uncertain inputs (Ha et al. 2012; Feizizadeh et al. 2004). GSA is depended on perturbations of the entire parameter space, where input factors are examined both

Table 5 WSPM's Scenario II; ranks and degree of effectiveness of themes used in the RWH potentiality mapping of W. Dahab Watershed

Thematic layer (criterion)	RWH potentiality class	Average rate (Rank) (R_c)	Weight (W_c)	Degree of effectiveness (E)
Volume of annual flood (VAF)	I (Very high) II (High) III (Moderate) IV (Low) V Very low)	0.9 0.7 0.5 0.3 0.1	16	14.4 11.2 8 4.8 1.6
Average overland flow distance (OFD)	I (Very high) II (High) III (Moderate) IV (Low) V (Very low)	0.9 0.7 0.5 0.3 0.1	17	15.3 11.9 8.5 5.1 1.7
Maximum flow distance (MFD)	I (Very high) II (High) III (Moderate) IV (Low) V (Very low)	0.9 0.7 0.5 0.3 0.1	10	9 7 5 3 1
Basin infiltration number (IF)	I (Very high) II (High) III (Moderate) IV (Low) V (Very low)	0.9 0.7 0.5 0.3 0.1	10	9 7 5 3 1
Drainage density (DD)	I (Very high) II (High) III (Moderate) IV (Low) V (Very low) V (Very low)	0.9 0.7 0.5 0.3 0.1	12	10.8 8.4 6 3.6 1.2
Basin area (BA)	I (Very high) II (High) III (Moderate) IV (Low) V (Very low)	0.9 0.7 0.5 0.3 0.1	11	9.9 7.7 5.5 3.3 1.1
Basin slope (BS)	I (Very high) II (High) III (Moderate) IV (Low) V (Very low)	0.9 0.7 0.5 0.3 0.1	12	10.8 8.4 6 3.6 1.2
Basin length (BL)	I (Very high) II (High) III (Moderate) IV (Low) V (Very low)	0.9 0.7 0.5 0.3 0.1	12	10.8 8.4 6 3.6 1.2

individually and in combination (Ligmann-Zielinska 2013). Variance-based GSA has been used in this context, where this approach is recognized as one of the most proper procedures for qualifying the factors' weights of the WSPM (Saltelli et al. 2000; Saisana et al. 2005). The aim of variance-based GSA is to quantitatively determine the weights that have the most effect on model results, in this case the RWH categorization is computed for each cell of the basin area by the decisive parameter. With this method, we aim to create two sensitivity measures: first order (S) and total effect (ST) sensitivity index.

The importance of a given input factor (X_i) can be measured via the so-called sensitivity index, which is defined as the fractional contribution to the model output variance due to the uncertainty in (X_i). For (k) independent input factors, the sensitivity indices can be computed by using the following decomposition formula for the total output variance ($V(Y)$) of the output (Y) (Saisana et al. 2005) (Eqs. 4–6):

$$V(Y) = \sum_i V_i + \sum_i \sum_{j>i} V_{ij} + \ldots + V_{1,2,\ldots k} \quad (4)$$

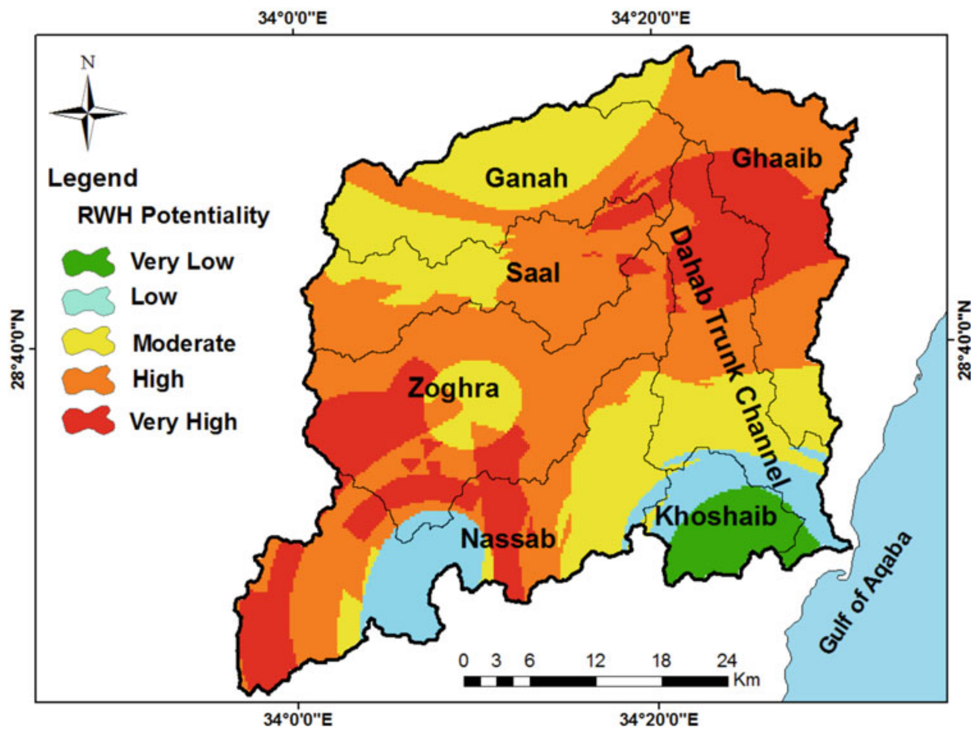

Fig. 28 WSPM map of Scenario II showing the RWH potentiality of W. Dahab Watershed

Table 6 RWH potential classes resulted from the WSPM's Scenario II map

RWH potentiality map					
RWH potentiality class	Very low	Low	Moderate	High	Very high
Area (Km^2)	156.64	292.66	442.45	881.19	298.85
Area % relative to the total watershed area (Total watershed area: 2071.75 Km^2) (%)	7.56	14.13	21.35	42.53	14.42

$$V_i = V_{xi}\{E_{x-i}(Y|X_i)\} \tag{5}$$

$$V_{ij} = V_{xixj}\{E_{x-ij}(Y|X_i, X_j)\} - V_{xi}\{E_{x-i}(Y|X_i)\} - V_{xj}\{E_{x-j}(Y|X_j)\} \tag{6}$$

A partial variance V_i represents the repeated variation of a single criterion (i) (i.e., one of the eight model criteria) that affects the other model criteria, which constitute the inputs of the WSPM. In other words, one of the WSPM eight parameters is changed while the rest remains constant. However, in Eq. 6, higher order effects ($V_{1,\ 2,\ \ldots\ p}$) are combined effect for two or more inputs. The partial effects can be calculated with special sampling schemes that are often computationally demanding (Saltelli et al. 2000).

Accordingly, the high-very high RWH potentiality classes and their total area (green columns), which are resulted from scenario I (equal weights to criteria) were compared to the Scenario III (unequal weighting), in which all criteria had been assigned an equal weight of 10% unless one criterion with 30%. Additionally, the percentage of variance in the total area of high and very high classes that resulted from scenario III was correlated with the scenario I (Figs. 37 and 38; Table 7).

Thus, it is observed that the BS has the highest percentage of variance value, followed by the MFD and Ba, whereas the least variance resulted from BL and VAF.

According to Fig. 38 and Table 7, the total of all variance ratios in the high-very high classes for the RWH potentiality in scenario III for each criterion with respect to their areas in scenario I is 60.64%. Accordingly, the justified weight of each criterion was determined by dividing the variance ratio of each criterion by the summation of all variance ratios (60.64%) (Fig. 38; Table 7), for example, the justified weight of the BS could be obtained by dividing its variance ratio (23.39%) by the summation of all variance ratios (60.64%), which is equal to 38.57% (Table 7).

Accordingly, the justified or optimum weights of each thematic layer shown in Table 7 were used to build a new arithmetic overlay approach within the ArcGIS 10.1© for performing the WSPM. The new justified weights are: BS

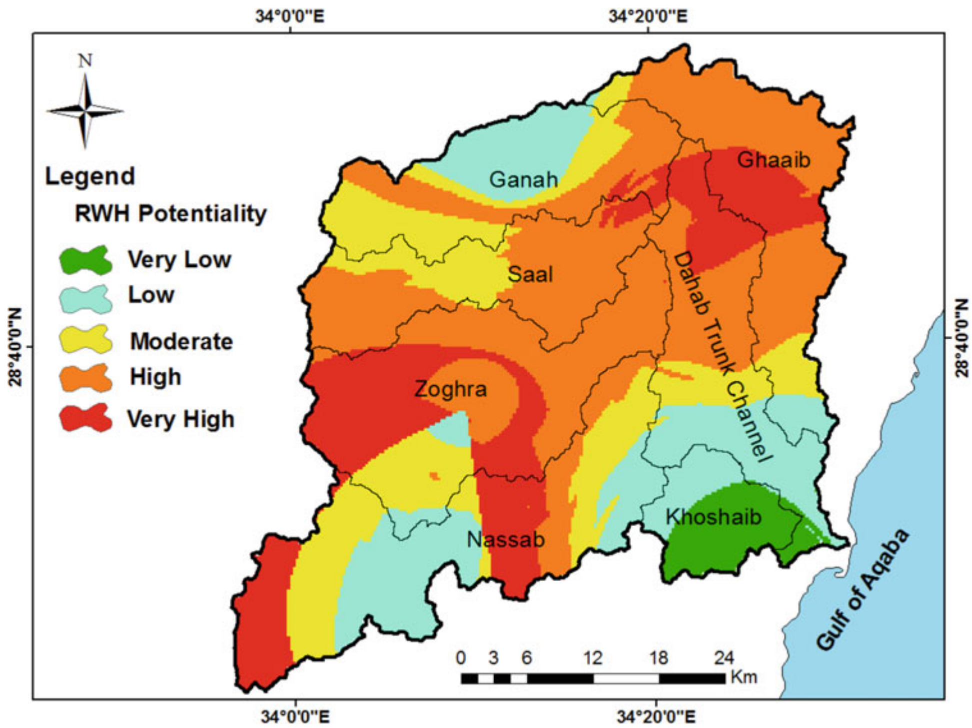

Fig. 29 WSPM map showing the RWH potentiality of W. Dahab (unequal weights: 10% for each thematic layer except the BA with 30%)

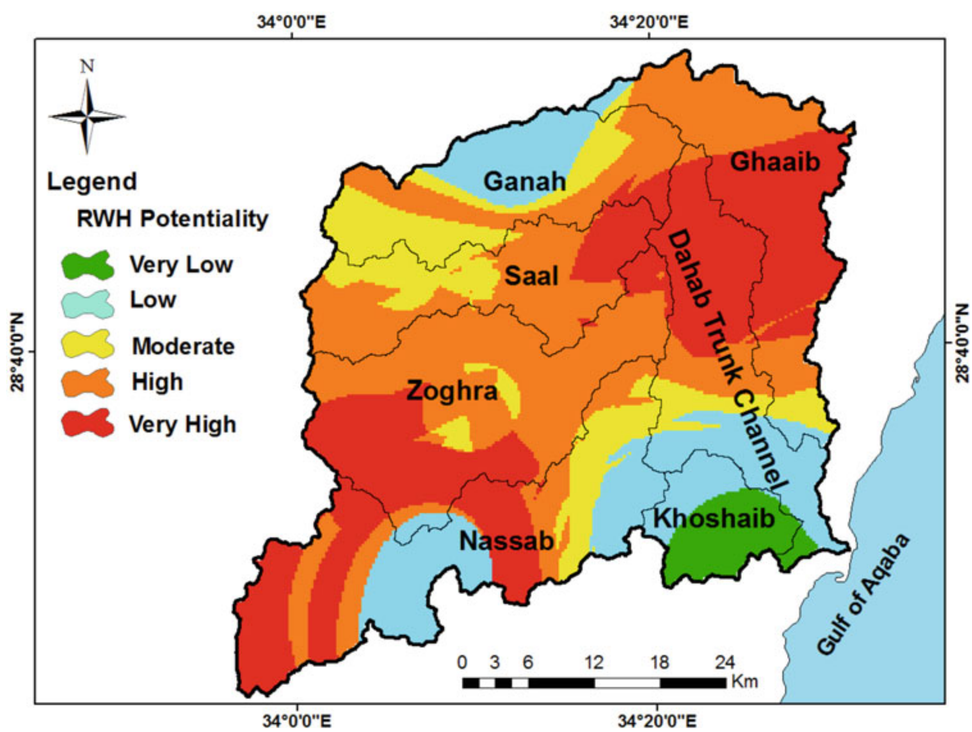

Fig. 30 WSPM map showing the RWH potentiality of W. Dahab (unequal weights: 10% for each thematic layer except the BL with 30%)

(38.57%), DD (8.71%), MFD (13.29%), VAF (1.86%), IF (8.67%), BL (7.44%), OFD (8.16%), and BA (13.29%). A WSPM output map with five classes ranging from the very low to the very high potentiality for the RWH was obtained. The spatial distribution of these classes relative to the total watershed area is 2.59% (very low), 8.85% (low), 14.7% (moderate), 58.27% (high), and 15.56% (very high) (Fig. 39; Table 8).

From the map produced by the audited weights (Table 8; Fig. 39), it could be concluded that the major area of W. Dahab is categorized as of high and very high for the RWH potentiality (58.27 and 15.56% of total watershed area,

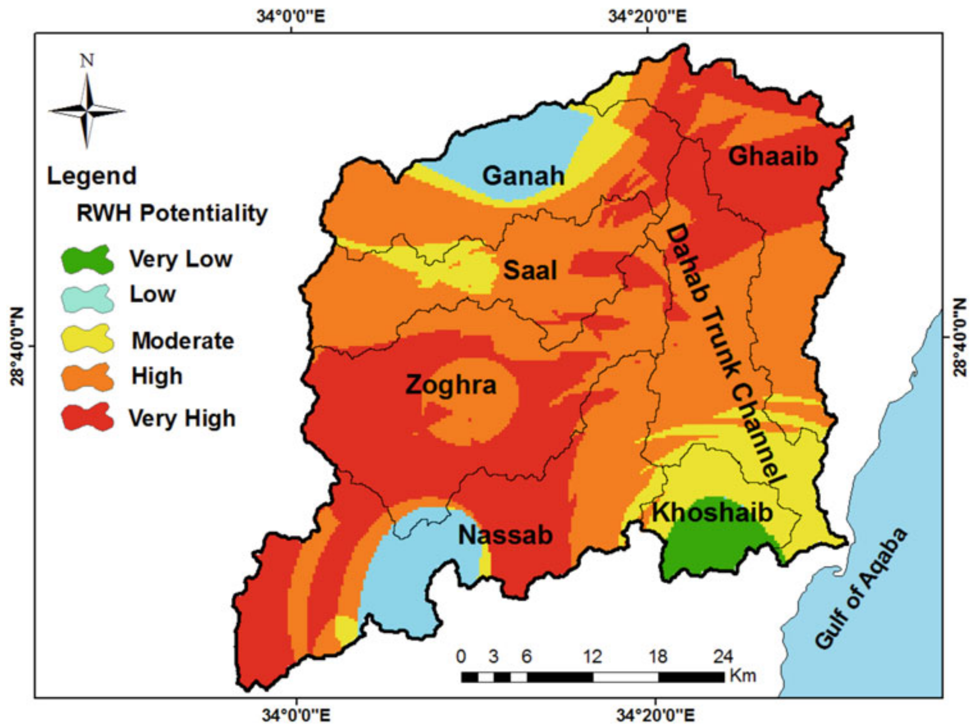

Fig. 31 WSPM map showing the RWH potentiality of W. Dahab (unequal weights: 10% for each thematic layer except the BS with 30%)

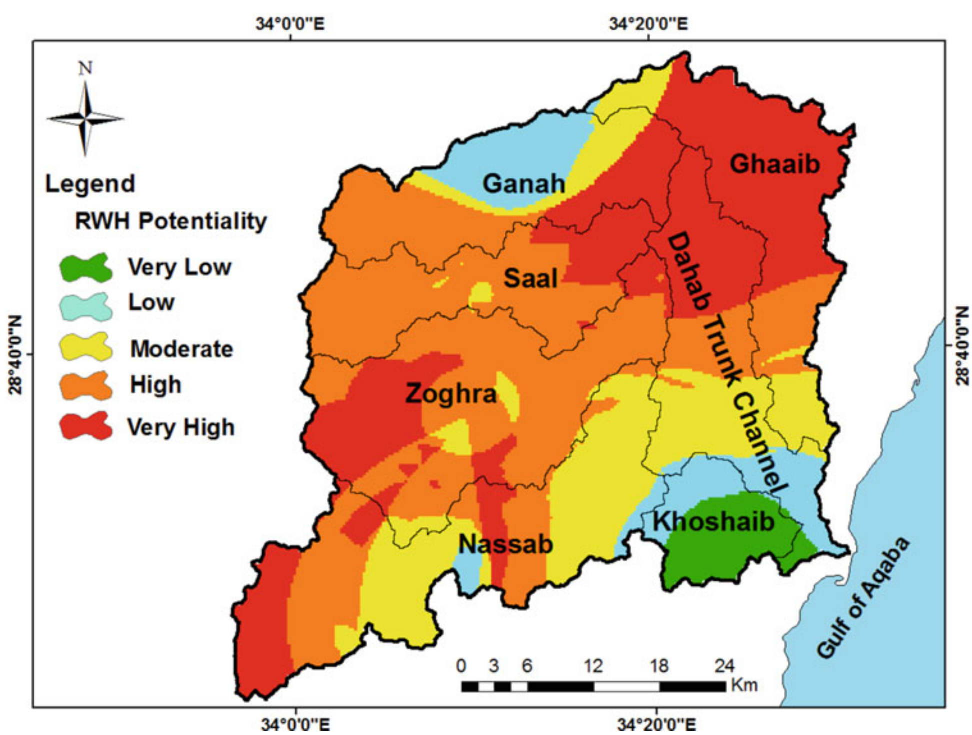

Fig. 32 WSPM map showing the RWH potentiality of W. Dahab (unequal weights: 10% for each thematic layer except the DD with 30%)

respectively), especially, in its northeastern, eastern, central, western, and southwestern parts, which are represented by El-Ghaaib, Dahab Trunk Channel, Zoghra, Nassab, Saal, Ganah, and Khoshaib sub-watersheds. The moderate class (14.7%), which is noticeably decreasing to low and very low (8.85 and 2.59%, respectively) are encountered in some areas in the upstream northwestern and southwestern parts of Saal, Ganah, Nassab, and Khoshaib sub-watersheds.

In general, the WSPM's scenario III map, which was audited by the sensitivity analysis, gives the results in favor of the other scenarios whether based on equal weights (scenario I) or those that were assumed by the authors

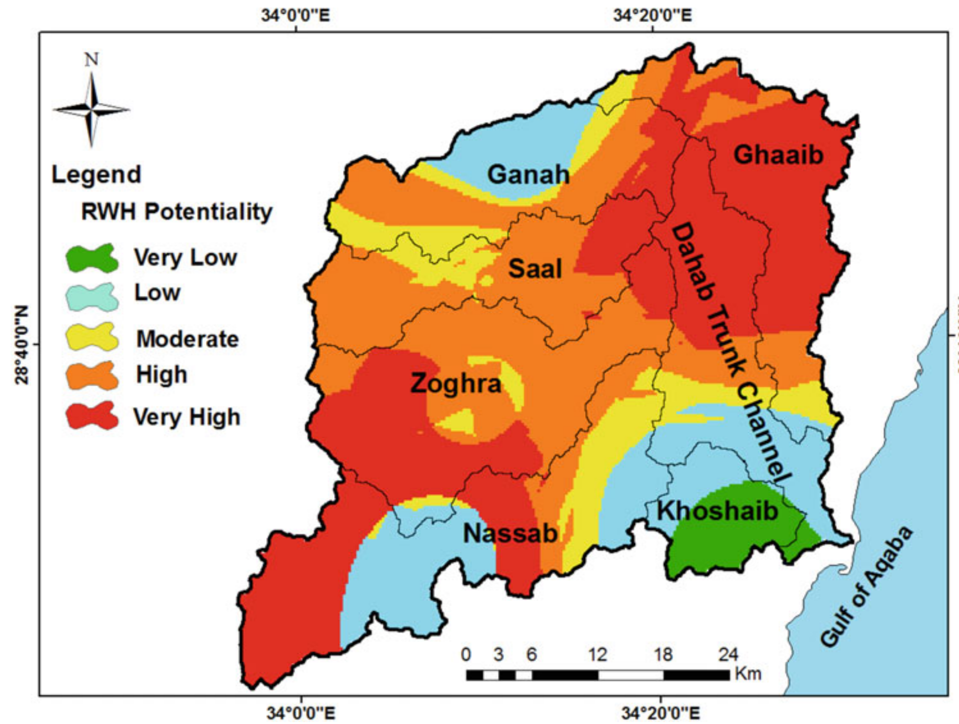

Fig. 33 WSPM map showing the RWH potentiality of W. Dahab (unequal weights: 10% for each thematic layer except the MFD with 30%)

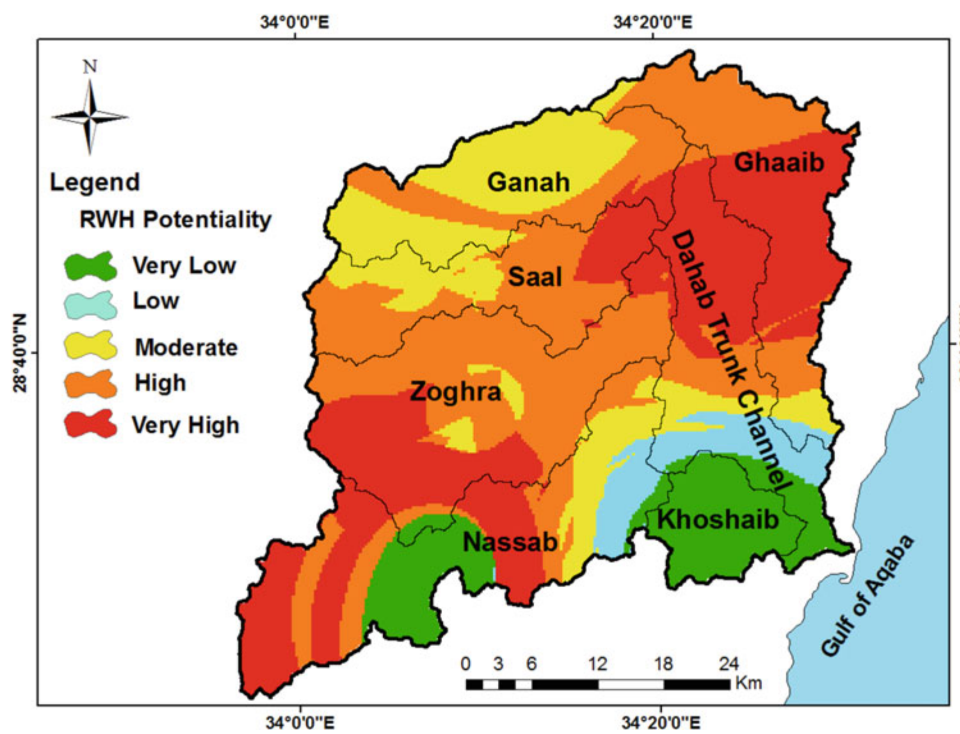

Fig. 34 WSPM map showing the RWH potentiality of W. Dahab (unequal weights: 10% for each thematic layer except the OFD with 30%)

Fig. 35 WSPM map showing the RWH potentiality of W. Dahab (unequal weights: 10 % for each thematic layer except the IF with 30 %)

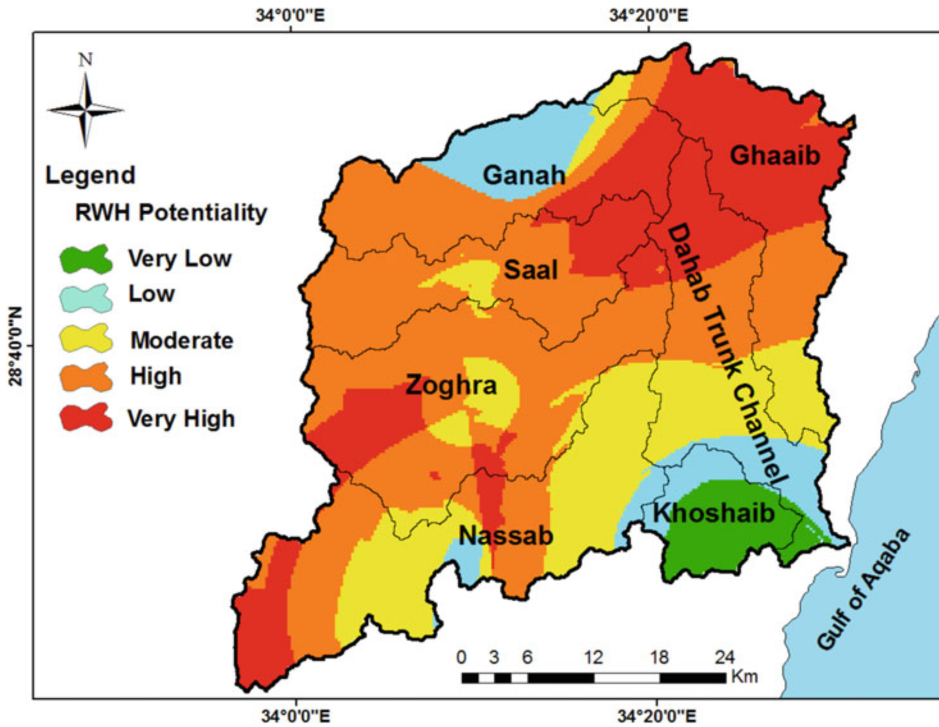

Fig. 36 WSPM map showing the RWH potentiality of W. Dahab (unequal weights: 10 % for each thematic layer except the VAF with 30 %)

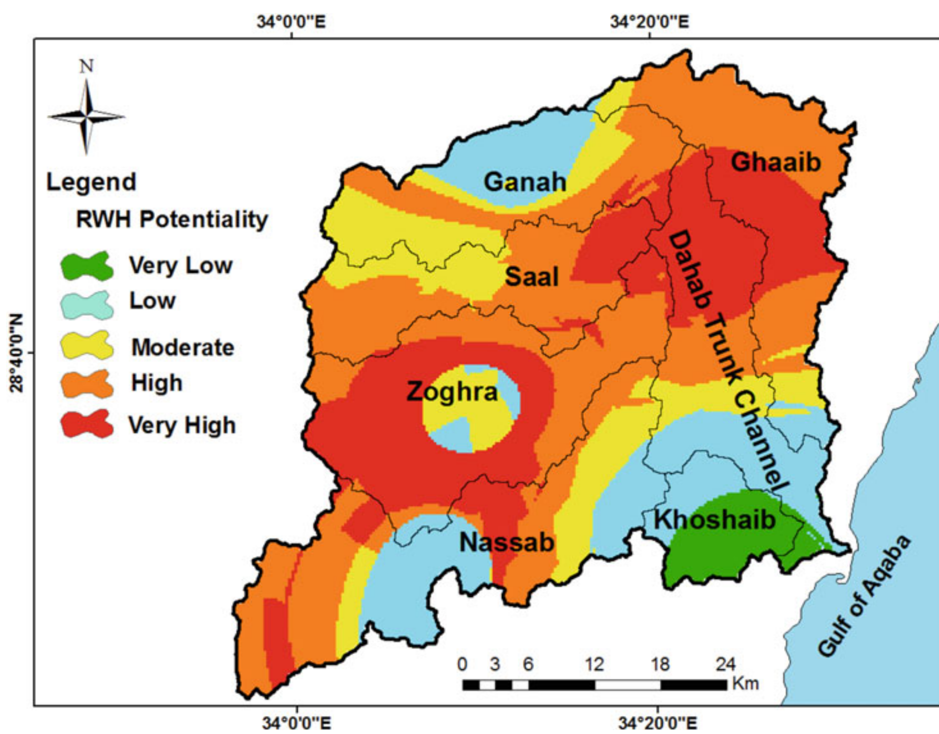

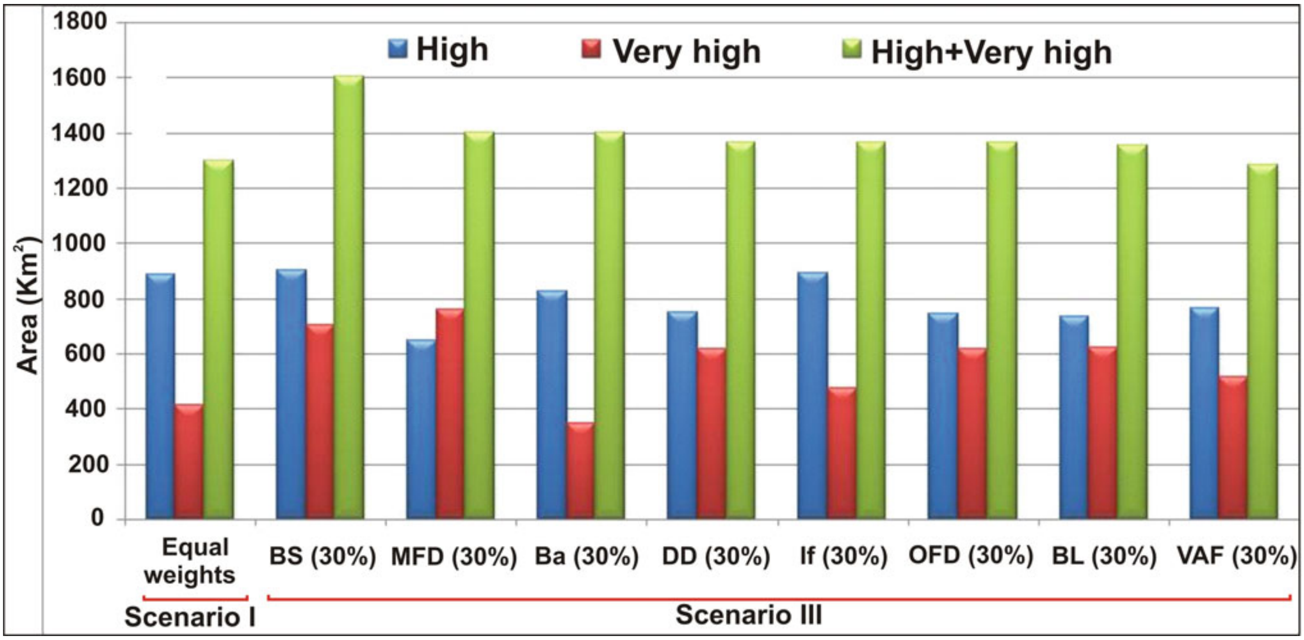

Fig. 3.37 Areas (in km^2) of the high-very high RWH potentiality classes and their summation in the two WSPM scenarios for W. Dahab Watershed

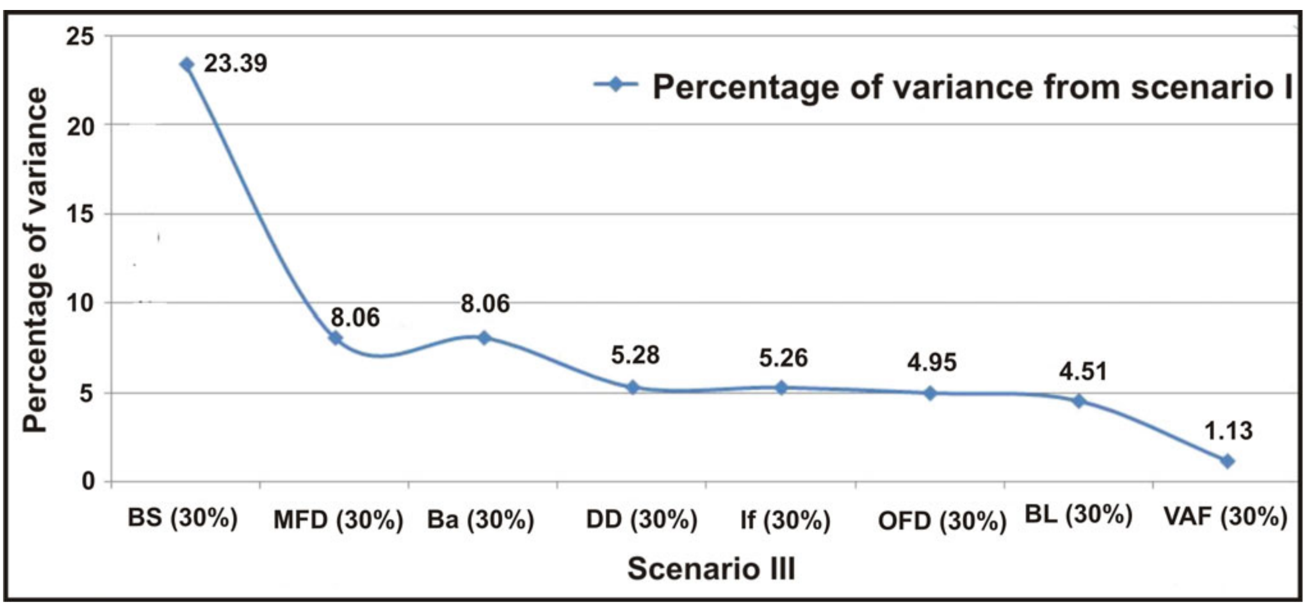

Fig. 38 A graph indicating the variance ratios of the high-very high classes in scenario III with respect to their areas in scenario I for W. Dahab Watershed

Table 7 The variance ratios and the justified weights of the WSPM's criteria used for the RWH potentiality mapping of W. Dahab

WSPM Criteria	BS	DD	MFD	VAF	IF	BL	OFD	BA
Variance ratio (%)	23.39	5.28	8.06	1.13	5.26	4.51	4.95	8.06
Justified weight (%)	38.57	8.71	13.29	1.86	8.67	7.44	8.16	13.29

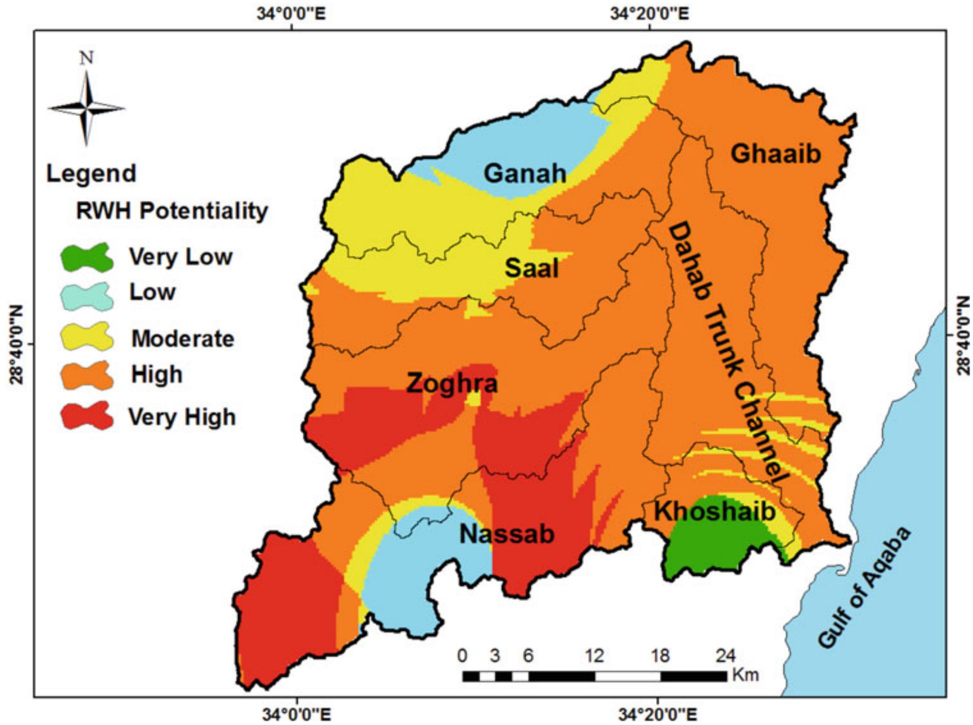

Fig. 39 WSPM map of scenario III showing the RWH potentiality of W. Dahab

Table 8 Areas of RWH potentiality classes resulted from the WSPM map of scenario III for W. Dahab

RWH Potentiality Map					
RWH Potentiality class	Very low	Low	Moderate	High	Very high
Area (Km^2)	53.75	183.54	304.71	1207.31	322.38
Area % relative to the total watershed area (Total watershed area: 2071.69 km^2) (%)	2.59	8.85	14.7	58.27	15.56

(scenario II). However, this gives very high credibility for the models used and, it confirms the performed field works and fulfills the local inhabitants' needs.

3.4 Proposed Action Plan for Applying RWH System

The present study proposed suitable locations for the construction of storage dams and ground cisterns to collect the runoff water. The moderate, high, and very high RWH classes are the most suitable areas for applying the RWH system to harvest any available quantities of runoff water and to mitigate the flash floods hazards. Four storage dams and five ground cisterns were proposed in optimum locations in the areas of moderate, high, and very high potentialities for the RWH (Fig. 40). The applied RWH system can help the decision-makers by proposing appropriate controlling systems for implementing runoff farming and rain-fed agriculture. Alluvial or wadi deposits in the main trunk channels of W. Dahab sub-watersheds will provide a good environment for the micro-catchment agriculture especially in the rainy seasons and for the establishment of new settlements in upstream and mid-stream areas of the studied watershed. Additionally, RWH has a direct impact on local Bedouin communities, which are the end users in these areas.

4 Summary and Conclusions

Wadi Dahab has very high importance in a new development in southeastern Sinai, for its touristic position and promising water resources. RS, WMS, and GIS techniques are modern research tools that proved to be highly effective in mapping, investigation, and modeling the runoff processes and optimization of the RWH. In the present work, these tools were

Fig. 40 Location map of proposed RWH systems of storage dams and cisterns in W. Dahab Watershed

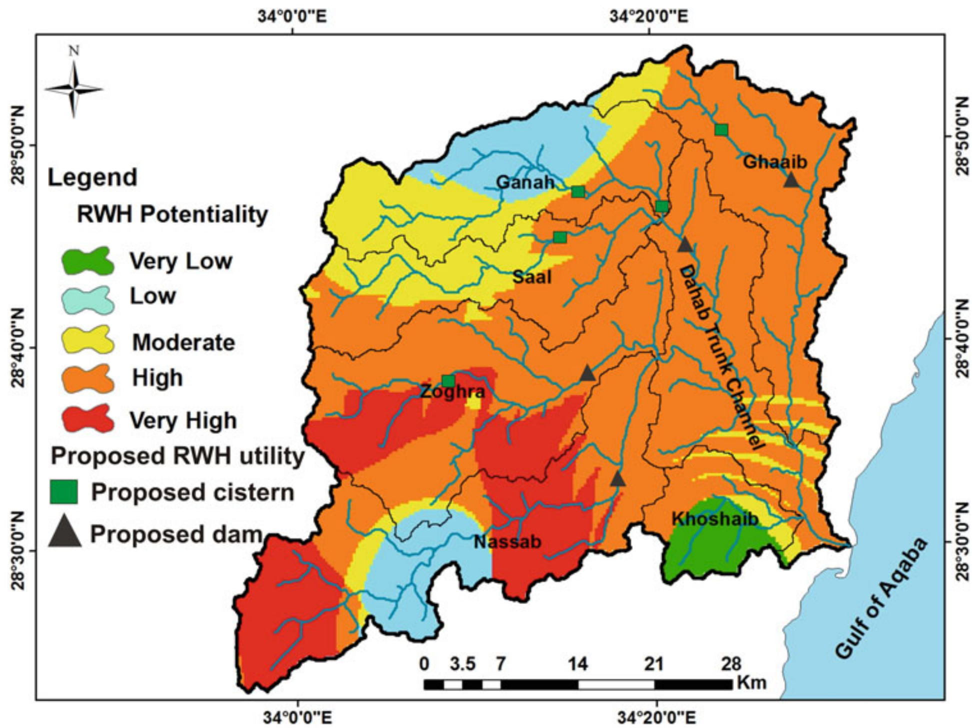

used to determine the potential sites suitable for the RWH in W. Dahab. The performed WSPM for determining the potentiality areas for RWH depended on the hydro-morphometric parameters of drainage density, infiltration number, maximum flow distance, overland flow distance, basin slope, basin area, volume of the annual flood, and basin length. The WSPM model was accomplished through three scenarios: equal criteria weights (scenario I), authors' judgment (scenario II), and weights justified by the sensitivity analysis (scenario III). The obtained WSPM maps for defining the RWH potentiality areas classified W. Dahab basin into five RWH potentiality classes ranging from very low to very high. There are good matches between the three performed WSPMs' scenarios in results for the very high and high RWH potentiality classes, which are very suitable for RWH applications.

There are good matches between the three performed WSPMs' scenarios in results for the very high and high RWH potentiality classes, which are very suitable for RWH applications. These classes are frequently represented generally by El-Ghaaib, Dahab Trunk Channel, Zoghra, Nassab, Saal, and Ganah sub-watersheds, which represent about 62.94%, 56.95% and 73.83% of the total area of the basin for scenarios I, II, and III, respectively. RWH utility system was suggested in selected optimum locations for harvesting runoff water and mitigating flash floods hazards.

Acknowledgments The authors wish to express their great gratitude to the science & technology development fund (STDF) for kindly funding and supporting the project entitled "Determination of Potential Sites and Methods for Water Harvesting in Sinai Peninsula by Application of RS, GIS, and WMS Techniques" where the present work is derived. Deep gratitude is also dedicated to the national authority for remote sensing and space sciences (NARSS) for providing the facilities needed for conducting the present work.

References

Aher, P. D., Adinarayana, J., & Gorantiwar, S. D. (2014). Quantification of morphometric characterization and prioritization for management planning in semi-arid tropics of India: a remote sensing and GIS approach. *Journal of Hydrology, 511,* 850–860.

AQUAVEO. (2008). Water modeling solutions. Support forum for sub-water-shed modeling system software (WMS) www.aquaveo.com.

Bisht, S., Chaudhry, S., Sharma, S., & Soni, S. (2018). Assessment of flash flood vulnerability zonation through Geospatial technique in high altitude Himalayan watershed, Himachal Pradesh India. *Remote Sensing Applications: Society and Environment, 12,* 35–47.

CONOCO (Continental Oil Company). (1987). Geological Map of Egypt (Scale 1: 500,000). CONOCO Inc. in Collaboration with Freie Universitat Berlin, ISBN 3-927541-09-5.

Dames, & Moore. (1985). The vegetation of boyagin nature reserve. Internal report of department of conservation and land management, Perth(unpubl.).

El Kiki, M. F., Eweida, E. A., & El Refeai, A. A. (1992). Hydrogeology of the Aqaba rift border province. *Proceeding of the 3rd Conference on Geology Sinai Development* (pp. 91–100). Egypt: Ismailia.

El Rayes, A. E. (1992). Hydrogeological studies of St. Katherine area, South Sinai. M.Sc. Thesis, Suez Canal University Faculty of Science (95p).

Elewa, H. H., Abu El-Ella, E. M., Ramadan, E. M., El Feel, A. A. (2015). Determination of Potential sites and methods for water harvesting in Sinai Peninsula by application of RS, GIS, and WMS techniques. Unpublished report, 744p.

Elewa, H. H., & Qaddah, A. A. (2011). Groundwater potentiality mapping in the Sinai Peninsula, Egypt, using remote sensing and GIS watershed-based modeling. *Hydrogeology Journal, 19,* 613–628. https://doi.org/10.1007/s10040-011-0703-8.

Elewa, H. H., Qaddah, A. A., & El-Feel, A. A. (2012). Determining potential sites for runoff water harvesting using remote sensing and geographic information systems-based modeling in Sinai. *Journal of Environmental Sciences, 8,* 42–55.

Elewa, H. H., Ramadan, E. M., & Nosair, A. M. (2014). Water/land use planning of Wadi El-Arish Watershed, Central Sinai, Egypt using RS GIS and WMS techniques. *IJSER, 5*(9), 341–349.

Elewa, H. H., Ramadan, E. M., & Nosair, A. M. (2016). Spatial-based hydro-morphometric watershed modeling for the assessment of flooding potentialities. *Journal of Environmental Earth Sciences, 75,* 1–24.

Elewa, H. H., Ramadan, E. M., El Feel, A. A., Abu El Ella, E. A., & Nosair, A. M. (2013). Runoff water harvesting optimization by using RS, GIS and watershed modeling in Wadi El-Arish, Sinai. *The International Journal of Engineering Research and Technology, 2,* 1635–1648.

Faniran, A., & Ojo, O. (1980). *Man's physical environment* (p. 404). London: Heinemann Educational Books.

Feizizadeh, B., Jankowski, P., & Blaschke, T. (2004). A GIS based spatially explicate sensitivity analysis approach for multi-criteria decision analysis. *Computers & Geosciences, 64,* 81–95.

Finkel, H. H. (1979). Water resources in arid zone settlement. In G. Golany (Ed.), *A case study in arid zone settlement, the Israeli experience* (p. 567). New York: Pergamon Press.

Ha, W., Lu, Z., Wei, P., Feng, J., & Wang, B. (2012). A new method on ANN for variance based importance measure analysis of correlated input variables. *Structural Safety, 38,* 56–63.

Javed, A., Khanday, M. Y., & Ahmed, R. (2009). Prioritization of sub-watersheds based on morphometric and land use analysis using remote sensing and GIS techniques. *Journal of Indian Society of Remote Sensing, 37,* 261–274.

Lewis, M. A., Cheney, C. S., & Ódochartaigh, B. É. (2006). Guide to permeability indices. British Geological Survey Open Report, CR/06/160 N, 29p.

Ligmann-Zielinska, A. (2013). Spatially-explicit sensitivity analysis of an agent-based model of land use changes. *International Journal of Geographical Information Science, 27,* 1764–1781.

Montgomery, D. R., & Dietrich, W. E. (1989). Source areas, drainage density, and channel initiation. *Water Resources Research, 34,* 1907–1918.

Omran, A. F. (2013). Application of GIS and remote sensing for water resource management in arid area-Wadi Dahab basin–south Sinai-Egypt (case-study). Ph.D. thesis, Tübingen, University, Germany, 282p.

Paz-Kagan, T., Ohana-Levi, N., Shachak, M., Zaady, E., & Karnieli, A. (2017). Ecosystem effects of integrating human-made runoff-harvesting systems into natural dryland watersheds. *Journal of Arid Environments, 147,* 133–143.

Rahman, S., Khan, M. T. R., Akib, S., Che Din, N. B., Biswas, S. K., Shirazi, S. M. (2014). Sustainability of rainwater harvesting system in terms of water quality. *Hindawi Publishing Corporation e Scientific World Journal*, *2014*, Article ID 721357, 10 pages. http://dx.doi.org/10.1155/2014/721357.

Said, R. (1962). *The geology of Egypt*. Amsterdam: Elsevier.

Said, R. (1971). Explanatory notes to accompany the geological map of Egypt. *Geological Survey of Egypt*, (special paper 56, Cairo).

Said, R. (1990). *Geology of Egypt* (p. 722p). Balkema Pub: Rotterdam.

Saisana, A., Saltelli, A., & Tarantola, S. (2005). Uncertainty and sensitivity analysis techniques as tools for the quality assessment of composite indicators. *Journal of the Royal Statistical Society, 168,* 307–323.

Saltelli, A., Tarantola, S., & Campolongo, F. (2000). Sensitivity analysis as an ingredient of modeling. *Statistical Science, 15,* 377–395.

Shendi, E. H., Oada K. (1999). Groundwater possibilities of wadi El-Nasb basin, southeastern Sinai, Egypt. *Annals of the Geological Survey* of *Egypt*, *VXXII*, 403–418.

Strahler, A. N. (1964). Quantitative geomorphology of drainage basin and channel network. In V. T. Chow (Ed.), *Handbook of applied hydrology*. New York: McGraw Hill.

Van Griensven, A., Meixner, T., Grunwald, S., Bishop, T., Diluzio, M., & Srinivasan, R. (2006). A global sensitivity analysis tool for the parameters of multi-variable catchment models. *Journal of Hydrology, 324,* 10–23.

Vema, V., Sudheer, K. P., & Chaubey, I. (2019). Fuzzy inference system for site suitability evaluation of water harvesting structures in rainfed regions. *Agricultural Water Management, 218,* 82–93.

Yazar, A., & Ali, A. (2016). Water harvesting in dry environments. In *Innovations in Dry Land Agriculture* (pp. 49–98). https://doi.org/10.1007/978-3-319-47928-63.